3-24-2016

Space Object Self-Tracker On-Board Orbit Determination Analysis

Stacie M. Flamos

SPACE OBJECT SELF-TRACKER ON-BOARD ORBIT DETERMINATION ANALYSIS

THESIS

Stacie M. Flamos, Civilian, USAF

AFIT-ENY-MS-16-M-209

DEPARTMENT OF THE AIR FORCE
AIR UNIVERSITY

AIR FORCE INSTITUTE OF TECHNOLOGY

Wright-Patterson Air Force Base, Ohio

AFIT-ENY-MS-16-M-209

SPACE OBJECT SELF-TRACKER ON-BOARD ORBIT DETERMINATION ANALYSIS

THESIS

Presented to the Faculty

Department of Aeronatics and Astronautics

Graduate School of Engineering and Management

Air Force Institute of Technology

Air University

Air Education and Training Command

in Partial Fulfillment of the Requirements for the

Degree of Master of Science

Stacie M. Flamos, B.S.

Civilian, USAF

March 2016

AFIT-ENY-MS-16-M-209

SPACE OBJECT SELF-TRACKER ON-BOARD ORBIT DETERMINATION ANALYSIS

THESIS

Stacie M. Flamos, B.S.
Civilian, USAF

Committee Membership:

Eric D. Swenson, Ph.D.
Chair

William E. Wiesel, Ph.D.
Member

Nathan A. Titus, Ph.D.
Member

Abstract

Due to the United States' growing dependence on space based assets and the increasing number of resident space objects (RSO), improvement of Space Situational Awareness (SSA) capabilities is more necessary than ever. As a way to aid in this need, the Air Force Institute of Technology (AFIT) is developing the Space Object Self-Tracker (SOS) as a proof-of-concept experimental satellite for RSO precision tracking and collision avoidance system in Low Earth Orbit (LEO). Specifically, SOS will use Global Positioning System (GPS) position estimates for on-board orbit determination. Currently, SOS will use the Simplified General Perturbations-4 (SGP4) algorithm as its orbit determination algorithm. This research investigates the use of a modified Special Perturbations (SP) orbit determination algorithm as an alternative means for on-board orbit determination (OD) for the SOS experiment. The research is focused on evaluating performance gains and studying the effects of using GPS navigation solutions as the input observation data on the achievable accuracy of the SP algorithm. The SP OD algorithm was evaluated in testing both simulated and real world observation data. The position estimates generated by the SP algorithm from both GPS navigation solution observations and observations delivered in the J2000 inertial frame were analyzed to determine the effects of the SP algorithm's achievable performance. The accuracy of position estimates generated from the SP algorithm were also compared to those generated by SGP4 algorithm. Analysis leads to the conclusion that the SP algorithm will be beneficial in providing more accurate position estimates for observed GPS navigation solutions. However, the SP algorithm will require improvements to the dynamics modeled in the SP algorithm by specifically including more perturbations such as those due to air drag.

Acknowledgements

I would like to express my sincere gratitude to research advisor, Dr. Eric Swenson, for all of the support and guidance he has provided not only throughout my research but also throughout my entire academic career at AFIT. His advice and genuine interest in my career has led me to achieving a job I have always wanted. I would also like to thank my committee member, Dr. William Wiesel, for the vast amount of help he has given me throughout my research efforts by not only providing the algorithm that I worked on for this thesis but also giving me a breadth of knowledge in writing software and orbit determination methods. Thank you Dr. Wiesel for your patience with my tiny amount of experience in writing code and supporting me while on unpaid leave. I am also extremely grateful to my committee member, Dr. Nathan Titus, for taking time to come to AFIT from NASIC and provide me with his valuable feedback and expertise.

I would like to extend a special thank you to Matt Lippert and Chris Lommano for saving me from drowning in my inexperience with writing C and C++ code. With their help, I have gained an overwhelming amount of knowledge in software development and I never would have been able to complete this research without them.

Lastly, I would like to express my most sincere thank you to my family and my fiance. I could never have gotten through the last year and a half without their constant support, encouragement, and love.

Stacie M. Flamos

Table of Contents

Page

List of Figures

Figure Page

List of Tables

SPACE OBJECT SELF-TRACKER ON-BOARD ORBIT DETERMINATION ANALYSIS

1. Introduction

The Space Object Self-Tracker (SOS) is an experimental spacecraft payload that autonomously estimates its orbit from Global Positioning System (GPS) receiver data and using an on-board orbit determination algorithm. This chapter provides the background information that establishes the relevance of this thesis topic in the context of Space Situational Awareness (SSA). The methodology used to address these issues is discussed, as well as the limiting conditions and assumptions made throughout the research. The chapter concludes by providing an outline of subsequent chapters throughout this thesis.

1.1 Background Information

Since the era of the Cold War, the United States (U.S.) has become increasingly reliant on space-based capabilities. These capabilities play critical roles both economically and militarily. [1] Satellites can provide valuable intelligence about potential attacks, adversaries' weapons development and deployment, and verification of arms control treaties and agreements. [2] Space-based capabilities can also add extremely beneficial capabilities to the U.S.'s national security, such as the command and control of unmanned aircraft, precision-guided munitions, intelligence, surveillance, and reconnaissance (ISR), remote sensing, and connectivity to remote locations. [2] Many others realize the benefit of space based capabilities through the use of global transportation, banking and financial systems, communications, disaster management, and

the monitoring and utilizing of natural resources. [2]

With such a strong dependence on space, protecting these assets must be a priority. As of September 2015, there were 1,305 operational satellites in Earth orbit, with only 42 percent, or 549 satellites, of those belonging to the United States. [3] There is an increasing global need to be cognizant of the threat of an on-orbit collision between resident space objects (RSOs).

The number of RSOs is continuously increasing due to the growing number of orbital debris. Orbital debris is made up of any man-made object in orbit around Earth which no longer serves a useful function, including nonfunctional spacecraft, abandoned launch vehicle stages, mission-related debris, and fragmentation debris. [4] Even small pieces of debris can cause serious damage to a functional spacecraft since they are traveling at orbital velocities near 7 kilometers per second. [4] The amount of trackable debris, or pieces larger than 10 cm, is more than 21,000 pieces. However, there are hundreds of thousands of pieces smaller than 10 centimeter and millions smaller than 1 centimeter that can still cause significant damage. [2]

In order to maintain superiority in space and avoid potential collisions with the ever growing amount of space debris, the United States must maintain SSA. SSA can be defined in many ways, but broadly speaking SSA involves determining the position, function, and current status of objects in space. [5] One of the sole focuses of SSA is to avoid potential collisions between orbiting objects, also referred to as conjunctions. Conjunctions can be catastrophic for a functioning spacecraft and cause a significant increase in space debris. [1] In 2009, the American Iridium 33 and Russian Kosmos 2251 communications satellites collided, becoming the first hypervelocity accident between two intact artificial satellites in Earth orbit. The instance created an estimated 2,000 pieces of space debris that must be continually tracked for conjunctions analyses. [1] With the growing number of space capabilities in other countries, SSA not only

has to focus on tracking foreign military satellites, but must also now focus to combat the increasingly contentious space environment, with such devices as antisatellite (ASAT) weapons, communications jammers, and sensor dazzlers. [1] As an example of this growing technology, in 2007 China fired an SC-19 direct-ascent ASAT missile at its own weather satellite as a test, creating more than 3,000 pieces of debris. [1] In order to preserve and protect its assets, the United States must implement a robust SSA program.

Currently, the USAF conducts its space control mission through the U.S. Strategic Command's (USSC) Joint Functional Component Command for Space (JFCC Space). Under JFCC Space, the Joint Space Operations Center (JSpOC) is responsible for SSA. [6] Through the use of the Space Surveillance Network (SSN) tracking systems, which include radar and optical sensors, JSpOC is able to detect, track, and identify all RSOs in Earth orbit above the size of 10 centimeters in the Satellite Catalog (SATCAT). As part of tracking RSOs, JSpOC is also responsible for estimating the orbit of an RSO into the future through the use of propagation methods. [6] In order to propagate an orbit forward, the space object's former state and a dynamics model are necessary. The observation data collected from the SSN is used to calculate the former state of the object. [7] As the dynamics model, JSpOC uses Simplified General Perturbations Number 4 (SGP4) to complete the calculation of the orbit element set. This propagator uses an approximate series solution to the equations of motion to demonstrate how a spacecraft's state will change over time due to perturbations, or an outside force acting upon an orbiting object. [7, 8] However, the systems used to calculate the propagation data date back to the 1980s and are long past obsolete. [2] As long as these legacy programs are in use, the USAF will face restrictions on the number of space objects it can catalog and track, the speed and accuracy of calculations to determine potential on-orbit collisions and warn satellite operators,

and the ability to take full advantage of future SSA sensor technology. [2] Though the methods used by JSpOC for orbital tracking are effective, the next section discusses how these methods can be improved.

1.2 Motivation

Although the ground based methods used by the SSN to track RSOs have been successfully practiced for several decades, they can become limited by weather, solar blind spots, and their geographical location on the Earth which can interfere with their ability to track an RSO when it is in view of the tracking system. [1] In efforts to reduce the risk of some of these issues, modernization efforts such as the Space Fence and research experiments by the Air Force Research Laboratory (AFRL) are under way in both the SSN and JSpOC. [9, 10]

One of the modernization efforts of the SSN sponsored by the AFRL's Space Vehicle Directorate (AFRL/RV) is the Air Force Institute of Technology's (AFIT) Space Object Self-Tracker (SOS) experimental mission, which is one of many missions in AFRL/RV's Payload Alert Communications System (PACS) program. A PACS device will ideally be a self-sufficient, self-contained, low cost, low size, weight, and power (SWAP) auxiliary payload to aid in the identification and precision tracking of RSOs that can be attached to any Earth orbiting space-bound object prior to launch. [11] Orbit determination (OD) for PACS, including position and error data, will be completed on-board the spacecraft using GPS navigation solutions as the observation data. The resulting solution from the OD algorithm will be transmitted to the ground user through an existing satellite communications (SATCOM) system, such as Iridium, Globalstar, or Orbcomm. The GPS data can also be downloaded and processed on the ground to achieve a more accurate orbital estimate if desired. [12,13] Previous research on the PACS program [14] has shown that including a PACS on

future RSOs may improve orbit estimates and conjunction analyses compared to the methods currently implemented, especially for orbital debris and inactive RSOs. Also, adding PACS to future systems can alleviate workload strain on SSN resources.

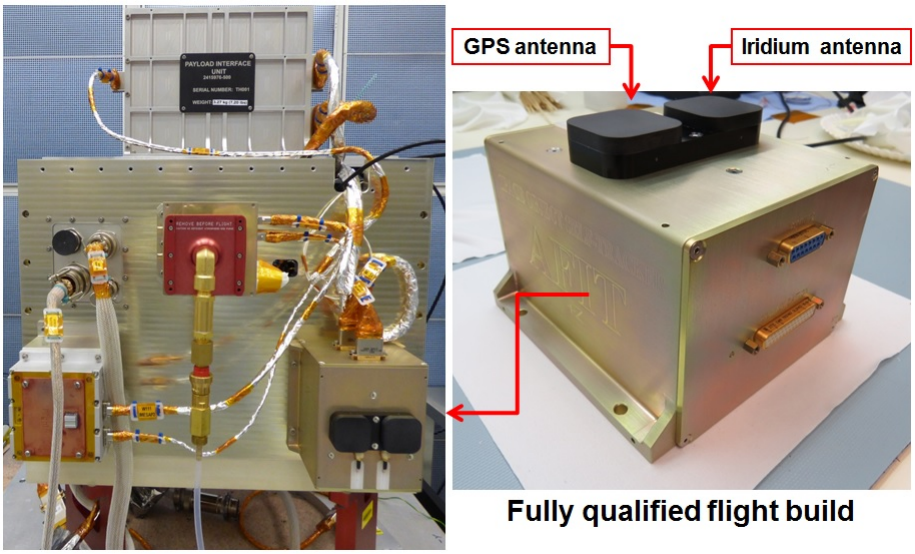

Figure 1. SOS Hardware Mounted on GPIM Host Vehicle [15]

As a technology demonstration of PACS, AFIT was sponsored by AFRL/RV to develop SOS shown in Figure 1, which is a small cube-shaped unit that was recently attached to a host satellite. However, SOS's mission differed from the PACS mission shown in areas such as being self-sufficient and small due to restrictions from the host vehicle. SOS will collect GPS data which will be used in OD on-board the spacecraft to estimate its orbit. Once a two line element set (TLE) has been estimated, SOS will utilize both the Iridium Network, a commercial LEO-based SATCOM network, and the Air Force Satellite Control Network (AFSCN) to downlink position estimates, telemetry, and mission data to the ground. The mission overview of SOS is shown in Figure 2. [11]

SOS was chosen as one of three auxiliary payloads approved by the Space Experiments Review Board (SERB) to fly as an experiment on a host satellite as part of the Department of Defense (DOD) Space Test Program (STP). [12] The host satellite

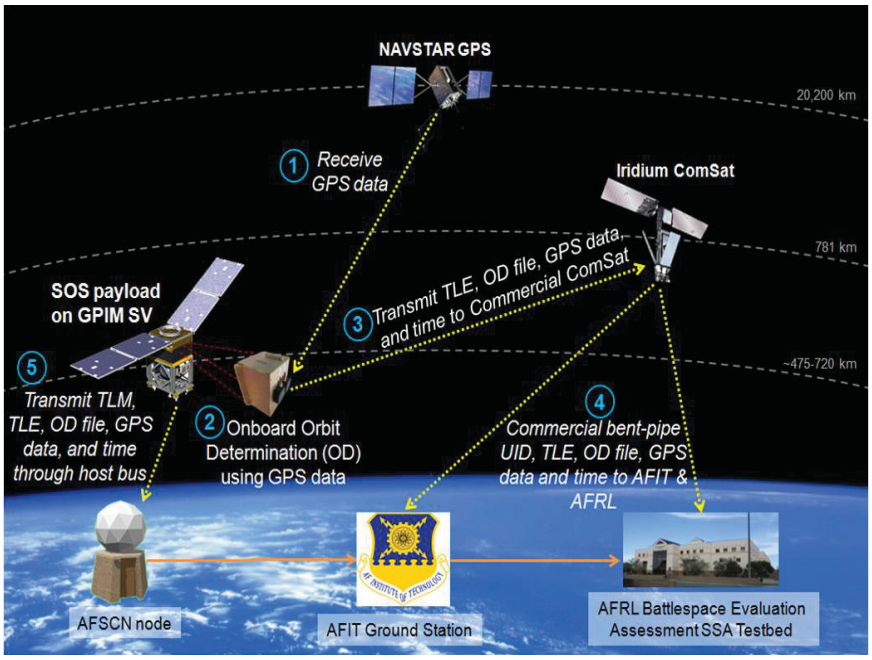

Figure 2. SOS Experimental Flight Mission OV1 Concept of Operations [11]

designated for SOS is a STP Standard Interface Vehicle (STP-SIV), whose primary mission is the National Aeronautic and Space Administration's (NASA) Green Propellant Infusion Mission (GPIM). The prime contractor for GPIM is Ball Aerospace and Technologies Corporation. The main objective for GPIM is to demonstrate a complete propulsion system for spacecraft attitude control and to utilize a new high-performance "green" propellant through a series of orbital adjustments and will act as the first U.S. demonstration of a nearly non-toxic monopropellant system. [16, 17] GPIM is currently scheduled to launch on a SpaceX Falcon Heavy LV tentatively in September of 2016. [16, 17] The launch will deliver the GPIM space vehicle to a 720 kilometer altitude, near-circular orbit at 24 degrees inclination and 192 degrees RAAN. [12] From there, the vehicle will demonstrate a series of orbital adjustments over a period of 81 days, shown in Table 1. [17] SOS will have opportunities to perform experiments at each of these altitudes, with additional opportunities once the GPIM experiments are over. STP-SIV is currently funded for one year, allowing SOS

approximately nine months to act as one of three primary experimental payloads. [13]

Table 1. GPIM Orbital Maneuvers [17]

	Altitude (km)	**Inclination (deg.)**
Launch Orbit	720 km	24
Maneuver 1	625	24
Maneuver 2	625	24.5
Maneuver 3	525	24.5
Re-entry Orbit	<500 (propellant dependent)	24.5

During operation, SOS will receive status messages once per second from the GPIM SV including a timestamp expressed in the number of GPS seconds since GPS week number rollover (August 22, 1999), the spacecraft position and velocity in ECI coordinates, the spacecraft attitude expressed as a quaternion, and the temperature of the spacecraft. [18] The SOS payload included a Antcom Corpoation Novatel OEM615 GPS receiver (Figure 3) and antenna (Figure 4) for collection of GPS data . [12] Using either the GPS data or information from the GPIM SV status message, SOS will perform on-orbit orbit determination to produce a "Super Two Line Element Set (TLE)." The "Super TLE," coined by AFIT faculty, students, and staff, contains a standard TLE describing the satellite's orbital parameters plus a file of residuals which demonstrate the position estimate errors. [13] Information from the "Super TLE" will either be transferred to the ground through Iridium or through the GPIM SV once in contact with AFSCN. Telemetry data and commands will also be passed through the GPIM SV. The GPIM SV will control SOS's power, as well as the capability to remove power from SOS's Iridium transmitter independently. [12] The flow of mission data is summarized in Figure 5. [18]

1.3 Research Focus

In the development of the SOS payload, there have been many technical challenges along the way, specifically with the on-board OD algorithm. Through previous

Figure 3. SOS GPS and Iridium Antenna Combination [12]

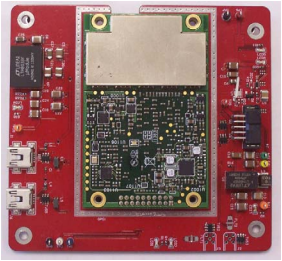

Figure 4. NovAtel OEM615 GPS Receiver on AFIT GPS Interface Board [12]

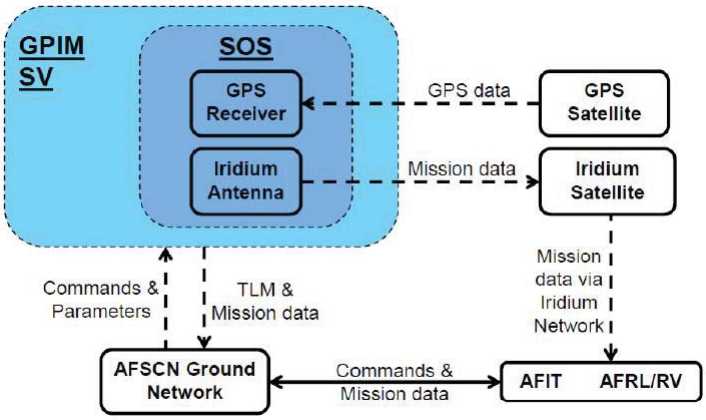

Figure 5. SOS Mission Data Flow to Ground through GPIM and Iridium [18]

research, it was demonstrated that the chosen OD algorithm for SOS, SGP4, will result in propagation position errors of around 2 kilometers per day. Using SGP4 does allow SOS to generate TLEs from GPS position estimates and achieve the "GPS data collection" objective as stated in Figure 6. However, the selection of SGP4 does not allow for a constructive comparison to the current tracking method accuracy of the SSN. [19]

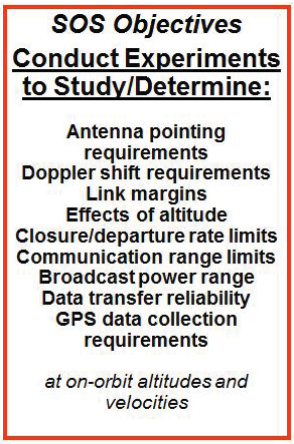

Figure 6. SOS Experiment Objectives [19]

This research investigates the use of a Special Perturbations (SP) orbit determination algorithm developed at AFIT as an alternative means for on-board OD for the SOS experiment. For this research, an existing implementation of the SP algorithm was modified to accept GPS observation data as its input into the SP algorithm. One of the expected outcomes of this research is the analysis of the effects of using the GPS observation data input in the SP algorithm. This research also focuses on comparing the accuracy of position estimates generated by the SP OD algorithm to the accuracy achieved by the SGP4 OD algorithm, which is currently in use as the SOS flight OD software. The accuracy of the SP orbit predictions is analyzed by answering the following investigative questions:

- How does the method of production of the truth model affect positioning accu-

racy?

- How sensitive is the SP OD algorithm to changing the input units of time?
- How sensitive is the SP OD algorithm to changing the input position reference frame?
- How does the choice of using physical or dimensionless units affect the efficiency and the positioning accuracy generated by the SP algorithm?
- How is the accuracy of the SP orbit predictions affected by adding perturbations from air drag or third body effects?

Using Analytical Graphics Incorporated (AGI) Systems Toolkit (STK) software, truth data for the simulation was produced at one of the orbital scenarios that SOS will incur due to the GPIM maneuvers described in Table 1. Through algorithms and the use of a Spirent GSS8000 GNSS Simulator, the orbit simulation was converted to GPS navigation solutions, including the time of observation and position of the spacecraft, for the SP software to input as observation data. By applying a non-linear least squares approach, the SP algorithm estimates the orbit of the satellite. The SP algorithm uses numerical integration for its propagation within the dynamics model, where the perturbing forces acting on the satellite are applied. The newly estimated orbit provides an updated state for the satellite at a given period of time. The position estimates and position residuals generated by the SP algorithm were compared to a truth model of the input data to analyze the achieved accuracy of the SP algorithm. The analysis completed for this research can determine the functionality and precision of processing raw GPS data sent from SOS to the ground using the SP OD algorithm, possibly lessening the load of needed ground-based observations from JSpOC. Results from this analysis may also demonstrate functionality of data collection and processing

capability if chosen to replace the existing OD algorithm for SOS and could have future implications for PACS implementations.

1.4 Assumptions and Limitations

The scope of this research was generated through assumptions and limitations. For testing of the SP algorithm, only ranges of orbital altitudes and inclinations likely to be experienced by the SOS experiment were evaluated. Orbit scenarios created by Jenson [12] are used to evaluate the SP algorithm in order to achieve a valid comparison between SGP4 and SP for the OD application. However, because of the higher accuracy level of SP, the J4 propagator in STK originally used by Jenson was changed to the more accurate High-Precision Orbit Propagator (HPOP) in STK to create the scenario truth models used for algorithm performance evaluation.

As previously stated, the first step in this research was to modify existing an SP algorithm to incorporate the use of GPS observation data. Because both the format of the GPS data and provided GPS sentence to inertial position conversion algorithm created by Wiesel were not modified for this research, this created limitations on the SP position estimation process. The format of the NMEA GPS sentences limits the input format precision for time, latitude, longitude, and altitude to be no greater than 0.01 seconds, 0.001 degrees, and 0.1 meters, respectively. When using this data to perform conversion calculations for an object traveling at orbital speeds, this formatting restriction can result in limitations to the achievable accuracy of the state estimates. Also, when completing the conversion from GPS sentences to an inertial frame position vector, the covariance data is assumed to be all equally accurate and does not include values such as dilution of position provided by the GPS receiver.

Since the main efforts of this thesis were spent on updating the SP algorithm to allow for GPS observation data input, improvements to the incorporated dynamics

model used in the SP algorithm were not addressed in this thesis and are suggested as future work. For example, the dynamics models used for this research did not include perturbation effects caused by the third body motion of the Moon or Sun since the altitudes chosen for analysis were likely to not show these effects. Also, perturbations caused by air drag are not included in the SP dynamics model at this time but should be added as future work.

1.5 Thesis Overview

This thesis is divided into five chapters. Chapter I establishes the background and significance of the topic to be researched, as well as the scoping assumptions and limitations. Chapter II provides a literature review that discusses complementary information relevant to this thesis topic to include: satellite tracking methods, orbit determination, time standards, and prior mission and experiments related to this research. Chapter III describes the methodology used to model, simulate, and analyze the problem. Chapter IV presents the interpretation and analysis of the experiment results, which characterizes the performance of the orbit determination algorithm and the time it took to complete it on different types of hardware. Chapter V summarizes the conclusions and recommendations from the experiment and provides a discussion of recommended future applications.

2. Background

This chapter presents a literature review of relevant background information such as different types of orbital tracking methods, including those used by JSpOC and satellite-to-satellite tracking. Also, topics such as perturbing forces, estimation theory, and propagation methods are introduced to provide background for discussing orbit determination methods used in this research and to describe how this research differs from what has been done previously. Because of the abundance of difficulties produced by the variety of methods used to represent time used through the algorithms in this research and those currently on SOS, different types of time standards are also addressed. Previous efforts related to the work completed in this thesis are also discussed.

2.1 Tracking Methods

This section discusses and compares two types of methods used for tracking space objects: ground based and satellite-to-satellite. The JSpOC detects, tracks, and identifies all artificial objects in Earth orbit through the use of radar and optical telescope surveillance sensors. [6] JSpOC astoundingly monitors over 46 trillion cubic miles between the Earth and the geostationary belt. [1] However, according to Morton [9], the technology being used at JSpOC is quickly approaching end of life. The need for more advanced forms of tracking are becoming necessary as SSA was not the primary purpose that these tracking methods were originally built for. Satellite-to-satellite tracking, through the use of systems such as the GPS, is an alternative to JSpOC ground-based methods. Using GPS to estimate the positions of space objects allows for more tracking data to be used in orbit estimation. Figure 7 displays object population in orbit around Earth. With the excessive amount of man-made debris and

space objects orbiting Earth, it is extremely important for effective tracking methods to be implemented.

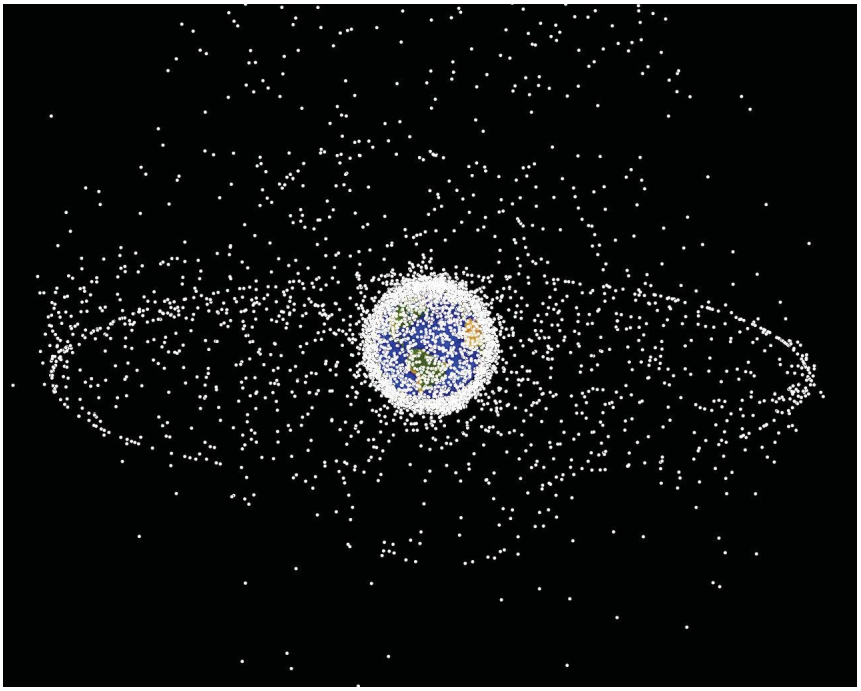

Figure 7. Geosynchronous and LEO Orbital Debris Around Earth [20]

2.1.1 JSpOC Tracking Methods

According to Baird, as of 2013 JSpOC was tracking more than 21,000 Earth orbiting objects greater than 10 cm. However, there are still at least 500,000 pieces of debris between 1-10 cm and an estimated amount of millions of pieces smaller than 1 cm. [1] JSpOC is responsible for charting the positions for orbital flight safety as well as predicting objects reentering the Earth's atmosphere with the objective of collision avoidance. [6] Due to the high velocities of the objects moving in space, typically several kilometers per second, even small pieces of debris can cause catastrophic damage to a satellite. [1] In order to form the Satellite Catalog, a listing of the numbers, types, and orbits of all tracked objects in space, JSpOC uses a system called the SSN. The SSN is worldwide network of 30 space surveillance sensors as

shown in Figure 8.

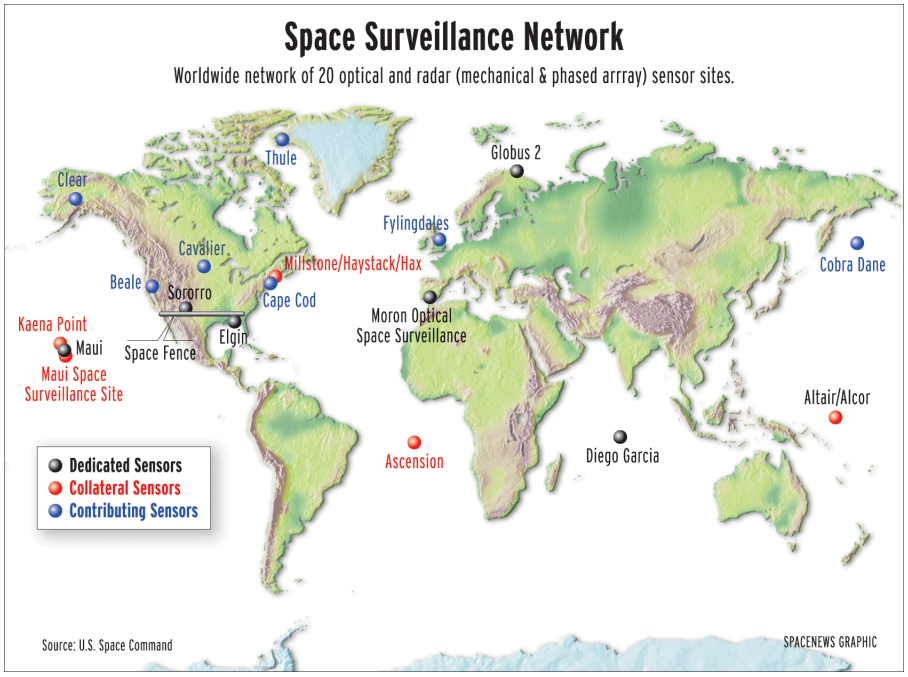

Figure 8. JSPoC Space Surveillance Network (SSN) [21]

JSpOC uses SSN to collect between 380,000 to 420,000 observations per day. Using these sensors, JSpOC spot checks space objects and uses a predictive approach rather than tracking them continually due to the limits of the SSN and the large number of items to be tracked. [6] Using the data collected from the SSN, JSpOC uses a series of algorithms, which are out of the scope of this discussion, to turn it into a set of parameters called TLEs. Each TLE describes the locations and velocities of an object in orbit using the six Keplarian parameters and state vectors, describing an orbit using a Cartesian coordinate system. [2]

2.1.1.1 Ground Radar Systems

SSN uses two types of ground-based radars: conventional and phased-array. Conventional radars use either fixed antenna or movable tracking antennas to emit a narrow beam of radiofrequency (RF) energy toward a satellite, then collects the re-

turned energy to compute the instantaneous location and velocity of the satellite. The conventional radar also uses this beam to follow the satellite's motion in order to continue collecting data. Examples of conventional radars can be found at the Reagan Test Site in Kwajalein Atoll and the Haystack Millstone facility at the Massachusetts Institute of Technology Lincoln Laboratory. On the other hand, phased-array radars can scan large areas of space in a fraction of a second in order to track multiple satellites simultaneously. The radar can scan at very high speeds, since the radar is steered electronically with no moving mechanical parts. Cavalier Air Force Station in North Dakota and Eglin Air Force Base in Florida house two examples of phased-array radars. [6]

Originally, the US Army built and operated conventional radars such as the ALTAIR complex between 1968 and 1970 with the purpose of simulating Soviet radar capabilities. As time went on, it became apparent that these radar systems could be used for the SSA mission. Through the use of cooperative agreements between U.S. government entities, the current SSA network was developed and used for a variety of missions. Currently, efforts to expand this cooperation globally with friendly nations and commercial entities are in progress in order to increase efficiency within the space environment. The creation and installation of a S-Band Space Fence is a prime example of this cooperation in progress. [1]

2.1.1.2 Optical Systems

Optical systems are also essential contributors to the satellite tracking mission, especially in tracking deep space objects. These types of systems are made up of telescopes linked to video cameras and computers. In order to generate tracking data, the video cameras feed pictures they collect from space into a nearby computer that controls a display scope. Using the same process as video cameras, the image is

then transposed into electrical impulses and recorded on magnetic tape, which allows the image to be recorded and analyzed in real time. [6]

The Ground-Based Electro-Optical Deep Space Surveillance (GEODSS) system tracks space objects as small as a basketball more than 20,000 miles away in space and has operational sites in New Mexico, Hawaii, and Diego Garcia. Another important optical asset is the Space Surveillance Telescope, located at the White Sands Missile Range near Socorro, New Mexico. This ground based optical instrument demonstrates three times better accuracy than GEODSS and captures more than 1 terabyte of data per night. It can also scan the geostationary orbit belt several times per night and search an area in space equal to the size of the United States in seconds. [1]

Because of the limitations of weather, solar blind spots, and geographical location of ground based systems, space based sensors are starting to be used such as the Space Based Surveillance System (SBSS) launched in 2010. [1] Space based sensors use infrared or optical sensors to either scan or quickly focus between targets without having to reposition the entire spacecraft. [6] Because of its higher altitude, this system can collect day or night over the entire geostationary belt without the limitations of being on the ground and improves the revisit rates of objects. [1]

2.1.2 Satellite-to-Satellite Tracking Method

Because ground-based satellite tracking encounters limitations due to only providing observations through spot checking, satellite-to-satellite tracking (SST) has started to become an alternative solution for our nation's satellites. Satellites equipped with a GPS receiver are able to collect much more position and velocity estimates than the JSpOC could ever receive using ground based tracking methods. This method has its own limitations, however. This tracking method only works for cooperative assets, since we are not able to receive GPS data from satellites of other nations or

commercial entities unless they give the U.S. government access to the data. Also, inactive satellites and orbital debris are not able to be tracked using SST. Because these limitations, the use of traditional JSpOC tracking methods will remain necessary. This section discusses a general overview of GPS and how GPS is used for SST.

2.1.2.1 Global Positioning System Overview

GPS is a space-based dual use radio navigation system that provides 24 hour positioning, velocity, and timing to military and civilian users. The GPS is maintained by the United States Air Force (USAF) and is a type of Global Navigation Satellite System (GNSS). [22] The continuous navigation signals produced by GPS are so accurate that time can be estimated to within a millionth of a second and velocity within a fraction of a mile per hour. [23] Position estimates vary depending on the frequencies used and errors introduced to the system, but can be accurate to the centimeter level if using differential GPS. [24] The GPS is made up of a minimum of 24 satellites in a constellation consisting of six orbital planes, with a minimum of four satellites per plane which orbit the Earth every 12 hours (i.e. two revolutions per sidereal day). [23] GPS satellites are currently launched from Cape Canaveral Air Station (CCAS), Florida into a 20,200 kilometer orbit using the Evolved Expendable Launch Vehicle (EELV). [23, 24] The design life of GPS satellites is seven and a half years; however, they currently are lasting more than ten to twelve years. [23]

Development of a United States' GNSS began with GPS's predecessors: The Johns Hopkins University (JHU) Applied Physics Laboratory (APL) Transit (also known as the Naval Navigation Satellite System), the Naval Research Laboratory's (NRL) Timation satellite program, and the USAF Project 621B. A multi-service Joint Program Office (JPO) was assembled in 1973 to develop the NAVSTAR GPS

and selected Rockwell International as the satellite contractor in June of 1974. The very first operational prototype of a GPS satellite was launched in 1978, followed by the first fully operational Block 2 version launched in February 1989. The GPS finally became a fully operation constellation of 24 Block 2 satellites in April 1995. [25]

The GPS was developed initially to allow smart weapons to precisely land on target and to create a unified navigation system among the branches of the U.S. military. However, the DOD recognized that this system could be extremely useful to the worldwide civilian community. In order to supply this technology while still maintaining national security, the USAF added a protective feature called "selective availability" (SA) that gave U.S. military and its allies significantly more precise satellite signals than civilian users. This capability worked to withhold full accuracy from U.S. enemies. By the time the GPS became fully operational, civilian and commercial users already had ten times more GPS receivers than the military, causing the request for the discontinuation of SA. President Clinton finally acknowledged this request in May of 2000 and directed the end of SA, allowing nonmilitary users access to more precise GPS signals. [25] Because of this, GPS is widely used and can be found in many everyday items. Even with the discontinuation of SA, GPS service is still split into two services for military security, called the Standard Positioning Service (SPS) and the Precise Positioning Service (PPS). PPS is intended for only authorized U.S. military and select government agency users and as the name implies is more precise than SPS which is designated for the general civil community. [26]

Space Segment The space segment of GPS consists of the satellite constellation and currently is made up of 31 operational satellites, where 24 operational satellites must be available 95 percent of the time. [24] The extra satellites can increase performance and are used to maintain coverage when satellites are serviced or decommissioned. Based on the four satellite/six orbital plane arrangement, at least

four satellites should be visible to the users from any point on Earth. [9] However, on June 15, 2011, a two phase GPS constellation expansion known as "Expandable 24," with the purpose to expand three of the baseline 24 constellation slots. This expansion began in January 2010 when maneuvers to reposition three GPS satellites were performed, followed by the maneuvering of 3 more satellites beginning August 2010. With this new optimal geometry of a 27-slot constellation, GPS coverage was increased for all users worldwide. [27]

In order to transmit ranging information and navigation data, the GPS satellites use a technique called code division multiple access (CDMA), which uses only two carrier frequencies referred to as L1 and L2. [26] Both frequencies are a multiple of the fundamental frequency f_0 of 10.23 MHz. Table 2 describes the relationship of each carrier frequency to the fundamental frequency and each wavelength. [28] The two frequencies are split by each satellite by assigning each satellite its own ranging code, or pseudo-random noise (PRN) codes, which were selected because of their low cross-correlation properties with respect to one another. [26]

Table 2. GPS Signal Description [28]

	Carrier Frequency (MHz)	**Multiple of f_0**	**Wavelength (cm)**
L1	1575.42	154	19.03
L2	1227.6	120	24.42

GPS uses two classes of codes, course-acquisition (C/A) code and precise (P) code. The C/A-code is intended for the initial acquisition of the GPS signal and is only transmitted on L1, while the longer P-code provides better performance since it has a higher chipping rate and is transmitted on L1 and L2. Due to the length of the P-code, it is more difficult to lock onto and requires accurate knowledge of time. In order to lock onto the P-code, C/A-code is usually locked onto first since it is so much shorter. Once the C/A-code is locked onto, the receiver can retrieve accurate

time information to lock onto the P-code. P-code in itself is unclassified, however, satellites normally only transmit a classified encrypted version known as P(Y) code. Table 3 summarizes the characteristics of both types of code. [28]

Table 3. Code Charactistics [28]

Parameter	**C/A Code**	**P-Code**
Chipping Rate [chips/sec]	1.023 x 106	10.23 x 106
Chipping Period [nsec]	977.5	97.75
Range of One Chip [m]	293.0	29.30
Code Repeat Interval	1 msec	1 week

Modernized GPS signals have also been developed in order to allow civilians more accurate navigation data (L2C and L5) and to add more security to classified military data (M). The GPS signal is also modulated with a 50 bit/sec navigation message. It is made up of five 300 bit "sub-frames," lasting six seconds each. Figure 9 displays the layout of each sub-frame. [28]

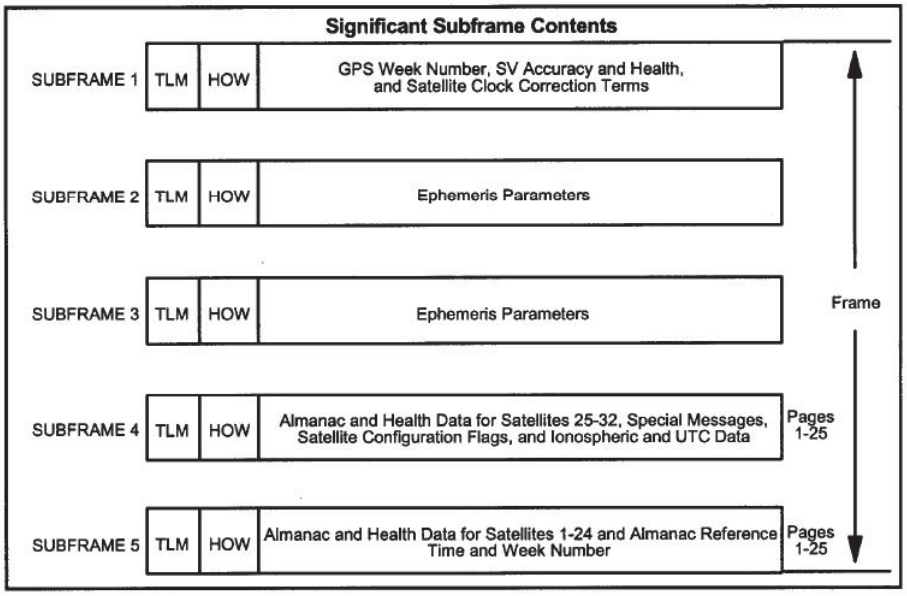

Figure 9. GPS Navigation Message Content [28]

User Segment The GPS user segment is composed of the user receiving equipment, typically referred to as a GPS receiver. The GPS receiver processes

the L-band signals transmitted from the satellites in order to determine the user's position, velocity, and time. The GPS receiver set can be broken down to five principal components: antenna, receiver, processor, input/output device, and a power supply. In the beginning, GPS receivers were very large and heavy devices. Today, however, GPS receivers can be found in most of the electronic products used every day, such as cell phones and bank ATMs. [26]

In order for the GPS receiver to calculate an estimate of the user's position, it requires navigation data and ranging code. The navigation data contained in the navigation data message allows the receiver to determine the location of each satellite at the time of signal transmission. Using the ranging code, the receiver can approximate the transit time of the signal which allows for the determination of satellite-to-user pseudorange.

To complete this process, the receiver must contain a clock to estimate Time of Arrival (TOA) ranging measurements from a signal transmitted by an emitter at a known location to reach a user receiver. Once this time is calculated, it is multiplied by the speed of the signal (either speed of sound or speed of light, depending on the type of signal being emitted) to estimate the distance between the emitter and receiver, known as the true geometric range. The receiver can estimate its own position by measuring the propagation time of the signal broadcast from multiple emitters. The TOA range measurements from four satellites are required to calculate a receiver's three-dimensional (latitude, longitude, height) location. If the receiver system time or height is accurately known, three satellites are required. [26]

The estimation of the range between the receiver and each GPS satellite has several types of errors. Pseudorange is the measurement of range as shown in Eq. (1). This calculation includes the true geometric range r, which is based off the true signal transmit time T_s and the time the signal would have been received without

errors T_u. The true geometric range is added to the speed of light c multiplied by the combination of receiver clock error δt_u, satellite clock error δt_{sv}, and additional error effects δt_D. [28]

$$\rho = r + c(\delta t_{\mathrm{u}} - \delta t_{\mathrm{sv}} + \delta t_{\mathrm{D}}) \tag{1}$$

The additional measurement errors that affect pseudorange include delays due to the ionosphere and troposphere, receiver noise and resolution error, multipath error, and hardware errors. Satellite position error also contributes to the solution but is not an actual measurement error. Figure 10 describes the effect of each type of error source on the range solution depending on the user (either SPS or PPS). PPS is less affected overall by measurement errors, mostly due to the use of both the L1 and L2 code measurements to remove ionospheric error. [28]

	Typical Range Error Magnitude [meters, 1σ]	
	SPS	PPS
Ionosphere	7.0	0.0
Troposphere	0.7	0.7
SV Clock & Ephemeris	3.6	3.6
Receiver Noise	1.5	0.6
Multipath	1.2	1.8
Total User Equivalent Range Error (UERE)	8.1	4.1

Figure 10. GPS Measurement Errors Table [28]

In order to correct or reduce these errors, several methods are used. Mapping functions are used to relate both ionospheric and tropospheric errors, although a model can also be applied to troposphere errors. Receiver noise can be filtered out of the system. Precise orbits obtained through the National Geodetic Survey can be used as a truth reference to reduce broadcast ephemeris errors. Through the use of the multiple channels (PRN code) and frequencies (L1 and L2), hardware errors can

be reduced. Multipath error mitigation can be completed through several approaches, including the use of different antennas, carrier-phase smoothing, the use of multiple receivers, or modeling the environment around the antenna. [28]

Control Segment The control segment is a global network of ground facilities responsible for tracking GPS satellites, monitoring their transmissions, performing analyses, and sending commands and data to the GPS constellation. As of March 2015, the control segment includes a master control station, alternate master control station, 12 command and control S-band antennas, and 16 monitoring sites, shown in Figure 11. [29]

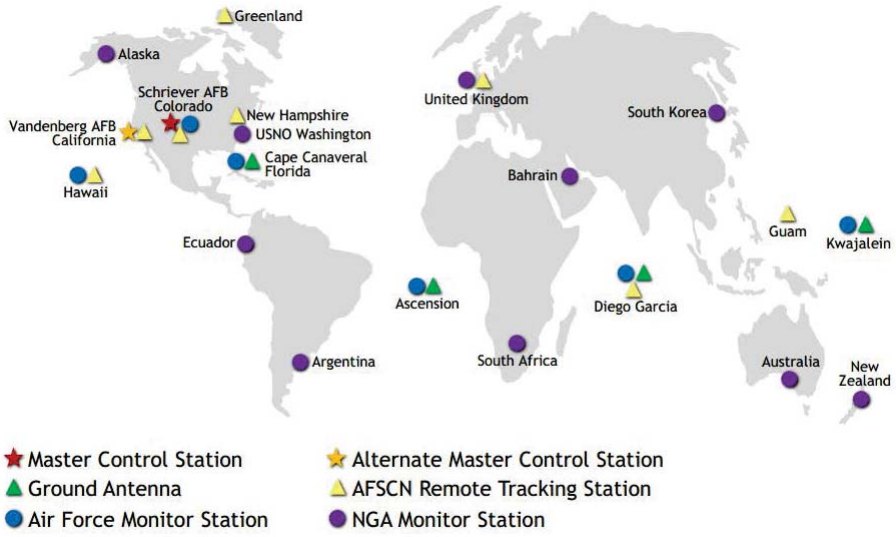

Figure 11. GPS Control Segment Locations [29]

The 50th Space Wing's 2nd Space Operations Squadron's GPS Master Control Station (MCS) at Schriever AFB is responsible for monitoring and controlling the GPS constellation. [23] The MCS generates and uploads navigation messages and maintains the state-of-health and accuracy of the constellation. Using navigation information received from the monitor stations, it computes the precise locations of the GPS satellites and uploads this data to the constellation. [29] Once the GPS

satellite knows its location, the capability for it to work with GPS receivers, whether on the ground or in space, which is to be discussed in the next section, becomes possible.

2.1.2.2 GPS Satellite-to-Satellite Tracking

With GPS's ability to provide continuous coverage, GPS SST is held superior to any ground-based tracking method. Because of this, most satellites in low Earth orbit are equipped with at least a single frequency GPS receiver that measures the course acquisition code and L1 phase. [30] Continuous precise tracking through GPS SST also allows for full observations of the satellite to observe orbit perturbations, especially for Earth gravity field models. [31] GPS SST requires GPS receivers that can handle different Signal Doppler and Doppler rates which are significantly higher in space due to the high speeds of low Earth orbiting satellites. Also, because GPS satellites are in view for much less time for LEO satellites than objects on the ground, receivers are required to compute solutions at much higher rates. [32] Even with these difficulties, the possibilities of GPS SST are still being pursued as an exciting technological advancement for the space community.

A GPS receiver acts as the main SOS payload along with a computer running OD algorithms to create a complete orbit determination test bed. There have been many other missions that have exercised this technique as well. The American/French altimeter mission TOPEX/Poseidon used GPS SST to investigate the accuracy potential offered by the observation system by processing the GPS SST data for precise orbit determination and gravity field model improvement. For the experiment, the satellite was flying at 1336 km at 66 degrees inclination with a repeating ground track of 10 days. The GPS receiver onboard used a six-channel dual frequency receiver that allowed for the use of continuous P- or C/A-code pseudo-range and carrier phase mea-

surements. The GPS satellites' ephemerides and clock parameters were introduced as fixed parameters to be used in the precise orbit computation with an approximate accuracy of 20 cm and 1 nanosecond. Due to using GPS SST, the TOPEX/Poseidon mission was able to produce an orbit solution with an accuracy of 10 centimeters in position and 2-3 centimeters in the radial direction, which was unprecedented for any altimeter mission. [31]

GPS SST has also been used to aid in the Gravity Recovery and Climate Experiment (GRACE), whose mission was to map the gravity field of the Earth using two satellites orbiting in the same plane in a low-low satellite-to-satellite tracking mode. The two satellites were flown at 300-500 kilometer altitude with a 22050 kilometer along-track separation at about 90 degrees inclination. Using a microwave ranging instrument, GRACE measured the range changes of the two satellites in order to compute the gravitational acceleration effects. The GPS receiver was used to continuously and accurately determine the orbits of the spacecrafts, as well as correctly register the gravitational field estimates in a terrestrial reference frame. Also, the low SST measurements encounter a singularity problem since the relative distance between the space vehicles is not adequate to determine the absolute position of each. The GPS measurements were necessary in order to alleviate the singularity. [33]

Data received from GPS SST can be used to perform orbit determination, either on-board or on the ground, and is especially beneficial for precise orbit determination. A very similar process is being tested for the SOS experiment. The main difference between previous GPS SST methods and what will be done on the SOS mission is that instead of using the raw GPS pseudorange data for POD, SOS will use navigation solutions computed by a GPS receiver in order to lessen the computational load of the SOS single board computer. The process for determining a satellite's orbit is discussed in the next section.

2.2 Orbit Determination

In order to determine the orbit of a space object, estimation methods require either JSpOC observations or on-board GPS data. Although the orbit can be determined at the specific time the measurements were collected with a sufficient amount of observation data which depends on the determination method used, factors called perturbing forces cause the space objects' orbit to slowly change with time. This section describes the perturbing forces that act on a space object, estimation theory, and specific propagation used in the space industry.

2.2.1 Perturbing Forces

The "two body problem" in orbital dynamics is known as the solvable force problem involving two masses interacting that can be described by a Newtonian point mass gravity model. However, there are many perturbing forces that act on an object in space. Normally, objects in the solar system are generally so widely separated that their gravitational fields essentially behave like a point mass field, which is why they can be treated as so in the two body problem. This same concept applies to the N body point mass problem, caused by the interaction between an orbiting body and a "third" gravitating mass. However, with the introduction of artificial Earth satellites, other perturbations are now of considerable significance on the objects, such as the effects of the Earth's oblateness, air drag, and the space environment effects. [8] In order to accurately estimate a satellite's orbit, perturbing forces such as the ones described in this section should be introduced when solving for the system's dynamics. Perturbing forces are a major component the OD algorithms used for the SOS experiment.

2.2.1.1 Gravitational Forces and the Effect of the Earth's Oblateness

Because of the Earth's rotation, it bulges at the equator causing its oblateness. Geographical characteristics such as continental blocks, ocean basins, and mountain ranges also are also assumed to cause deviations to the Newtonian point mass model. [8] Since the Earth is not perfectly spherical and does not have a uniform density, its gravitational field cannot be modeled with the entire mass concentrated at its center if accurate results are to be expected. [34]

Commonly, Earth's gravitational potential is modeled with a series of several potential terms that accurately describe the regional differences in the Earth's shape and density. The oblateness of the Earth, specifically at the equator, is the most significant deviation from the point mass model and is referred to as the J_2 term. The radius of the Earth at the equator is on average 20 kilometers greater than at the poles. [34] Therefore, there is a higher gravitational potential over the equatorial zone. Eq. (2) represents the potential term V_{20} of the first non-vanishing zonal harmonic in the geopotential expansion, where μ is the the standard gravitational parameter of the Earth, $R_\oplus$ is the equatorial radius of the Earth, J_2 is 0.001082 , r is the distance relative to the center of the Earth in spherical polar coordinates, and θ is the colatitude in spherical polar coordinates. [8]

$$V_{20} = \frac{\mu R_\oplus^2 J_2}{2r^3}(2\cos^2\theta - 1) \tag{2}$$

The oblateness of the Earth affects Earth-orbiting satellites in two ways. First, the extra mass around the equator of Earth creates a torque on the orbital plane, resulting in an effect known as the regression of the nodes. When the torque is integrated over the period of the entire orbit, it produces a gyroscopic effect causing the orbital plane

to precess around the Earth's spin axis. The precession rate can be examined in the right ascension of the ascending node (RAAN) Ω and is given in Eq. (3), where a, e, and i are the semi major axis, eccentricity, and inclination, respectively, and n is the mean motion. This results in a decreasing RAAN for prograde orbits. [34]

$$\dot{\Omega} = -\frac{3nJ_2R_{\oplus}^2}{2a^2(1-e^2)^2}\cos i \tag{3}$$

The oblateness of the Earth also affects elliptical orbits by rotating them within the orbital plane. This effect is referred to as the advance of the perigee, since it results in a change in the argument of perigee ω, as shown in Eq. 4. For low to moderate inclinations, this effect results in a positive change in ω. This effect is greatest for orbits with a small semimajor axis a or inclination i. [34] Each of these effects causes ω and Ω to change linearly with time. [34]

$$\dot{\omega} = -\frac{3nJ_2R_{\oplus}^2}{2a^2(1-e^2)^2}(\frac{5}{2}\sin^2 i - 2) \tag{4}$$

2.2.1.2 Air Drag

Although the atmosphere hundreds of kilometers away from the Earth can be considered nearly a vacuum, there still remains enough gas molecules to affect the motion of a spacecraft in the form of atmospheric or air drag, especially in low Earth orbit. Even though this effect is small, its accumulation over time eventually causes the spacecraft's orbit to decay and the spacecraft to reenter the Earth's atmosphere. [34] No natural object in the solar system orbits their primary body close enough to feel the effects of air drag, but the addition of artificial Earth satellites to the solar system creates the need for this effect to be examined. Artificial satellites also differ from natural orbiting objects because the ratio of total area to mass is normally very large, causing air drag to take effect on its orbit. [8]

The air molecules in space strike the spacecraft at such high speeds and at such low densities that they no longer behave as a fluid but as individual particles in the free molecular flow regime. As the air molecules hit the spacecraft and potentially bounce off, they transfer linear momentum through the inelastic collision proportional to the speed of the satellite with respect to the air. [8] Equation (5) represents the magnitude of the acceleration due to air drag a_d, where v is the magnitude of velocity of the spacecraft, ρ is the atmospheric density, C_d is a function of the satellites shape called the coefficient of drag, A is the projected area of the satellite as seen from the direction of motion, and m is the spacecraft mass. [34]

$$a_d = \frac{1}{2}\rho v^2 \frac{C_d A}{m} \tag{5}$$

Isaac Newton derived this form of the drag law, as he was under the impression that a fluid was a group of noninteracting particles. [8] The direction of this acceleration is opposite of the velocity vector. [34] The coefficient of drag, area, and mass of the satellite $\frac{C_d A}{m}$ may not typically be determined separately, therefore, this group of terms is referred to as the ballistic coefficient B^*. [8]

Air drag can be very difficult to predict for a satellite on orbit, mostly due to the ballistic coefficient and atmospheric density. The ballistic coefficient is dependent on the satellite's effective area to mass ratio, which is a function of the satellite's shape and attitude. Sources of changes in atmospheric density can be fairly well known in some cases, such as bulges over the equator, heating effects, and the diurnal bulge. Density becomes unpredictable in the exosphere due to the interaction with the Earth's radiation belts. Unexpected solar flares can expel a huge amount of energetic particles into the radiation belts, causing a sudden increase in air drag on low Earth orbiting satellites. The same kind of effect can be felt on a satellite due to changes in the magnetic field of the Earth. Because of all of this unpredictable

behavior, estimating a satellite's orbit into the future can be very unpredictable due to the effects of air drag. [8]

2.2.1.3 Radiation Pressure

The pressure of the sunlight itself can create a perturbing effect on artificial Earth satellites' orbits, although this usually only needs to be accounted for in very high accuracy work. The acceleration due to solar radiation pressure a_l, where a_l is a vector, can be found in Eq. (6).

$$\mathbf{a}_l = \frac{E}{c}\frac{A_g}{m}\frac{\mathbf{R}_s}{R_s^3} \tag{6}$$

The intensity of the sunlight depends on the distance from the sun R_s as an inverse square law, where R_s is also a vector. As light is reflected diffusely, the acceleration is directed away from the sun. The solar constant E is the amount of energy flowing through a 1 centimeter surface at 1 Astronomical Unit from the sun. The quantity $\frac{E}{c}$, where c is the speed of light, gives the momentum flow per unit area per unit time and is a small number. Similar to the coefficient of drag for air drag, the reflectivity factor g takes into account the different reflection directions due to the shape of the object. Just as g is similar to C_d, the group $\frac{Ag}{m}$ is similar to B^* in the drag equations as both depend on the area to mass ratio. This grouping accounts for the susceptibility of a satellite to radiation pressure. Because solar radiation pressure acceleration also has a dependence on the area to mass ratio, predicting its effect on a satellite's orbit into the future can become difficult. Other factors in making the prediction of solar radiation pressure acceleration include the effect of slipping into Earth's shadow, the Yarkovsky effect, and the Poynting-Robertson effect. [8]

2.2.2 Estimation Theory

Estimation theory originated in the application of the orbital tracking problem. [7] There are two primary components necessary in order to estimate an orbit, measurements of the object's former state and a dynamics model. Historically, estimation theory was purely deterministic, in that it was assumed that the dynamics model contained no error, but the information on the dynamical system was extracted from observations which do contain errors. This deterministic approach is used in Karl Friedrich Gauss' method of least squares. As new approaches of estimation theory were established, stochastic estimation, the assumption that both the measurement and dynamics include errors, started to be used with methods such as the Kalman Filter. [7]

Errors in measurements are unavoidable, as mistakes in observations and recording can occur and measurement instruments will never be perfectly designed and manufactured. Errors tend to follow the Central Limit Theorem, developed by Gauss. The overall instrument error can be described by a Gaussian function, no matter how small the errors are distributed, if the total instrument error is made up of very small error sources. The large amounts of small error sources do not dominate the total error. Most of the world's data comes from instruments that follow Gaussian statistics, however, non-Gaussian error statistics can be applied by introducing one of two large error sources. In practice, the central limit theorem is achieved by finding and eliminating all of the large error sources in an instrument until the point of diminishing returns is reached. The standard deviation describes how precise the instrument is and is a property of the instrument itself; whereas the accuracy of the data depends on how the instrument makes a measurement. Calibrating the instrument provides the instrument bias and standard deviation in order to determine the reliability of the measurements. [7]

Gauss established the first method of estimation theory with the development of the method of least squares. He summarizes the method as follows: "The most probable value of the unknown quantities will be that in which the sum of the squares of the differences between the actually observed and the computed values multiplied by numbers that measure the degree of precision is a minimum." [35] In layman's terms, the least squares method determines the most probable value of the state vector $\mathbf{x}$. The most probable value is the value that minimizes the sum of the squares of the residuals, or, the difference between the observed and computed measurement values. [35] The method of least squares can be applied to both linear and nonlinear systems. However, most dynamical systems behave nonlinearly, such as orbital dynamics. Not only are the dynamics of orbital motion nonlinear, but the observed quantities are also typically related to the system state by a nonlinear set of relations. For example, the relation between the classical orbital elements and azimuth observed by radar can only be described by a nonlinear relationship.

In order to complete the method of least squares, it is necessary to make an initial guess of the state vector $\mathbf{x}$, known as the reference trajectory $\boldsymbol{x}_{ref}(t_0)$. This reference trajectory is typically found using a few data points to solve explicitly for the trajectory and ignoring data errors. It is also required to define and linearize both the system dynamics, found from the solution to the equations of motion, and the observation data. Using this data, the state vector can be propagated to the observation time and residuals can be found for each data point. A new covariance matrix and state vector can be made with the found corrections and the process will continue until convergence has been achieved with the reference trajectory. The length of this process usually depends on the accuracy of the initial estimate of the reference trajectory. [7]

In the last several decades, a new interest has taken place in estimation theory,

which led to the development of new techniques such as the Kalman filter. This occurred due to the fact that the development of computers has made it possible to process large amounts of data to routinely produce estimates. This led to the field of stochastic estimation, which replaces the deterministic dynamics with random noise, or, errors in the data or state. Different types of filters were produced that use an estimation algorithm to extract the system state from observations with errors. [7]

Sometimes called the "optimal operator," the Kalman filter differs from Gauss' method of least squares in that both the observations and the dynamics are characterized by statements about their statistical behavior. The Kalman filter is known as a sequential estimation method, as it uses a previous estimate as the data input to a new estimator and improves the estimate sequentially. The previous estimates are used as the reference trajectory in the new estimates, whereas in least squares, it is assumed that all data is available and processes one large batch of data with a reference trajectory that must be "close enough" to the final estimate to ensure convergence. Because of this, sequential methods such as the Kalman filter requires far less iterations to converge on an estimate. However, the Kalman filter in itself is actually just a rearrangement of the least squares method. The Kalman filter requires both observational data and a covariance matrix; therefore it sometimes uses an initial run of least squares since it is incapable of self-starting. Without a legitimate initial estimate, the Kalman filter can produce a singular covariance matrix that the filter is incapable of getting rid of. When running this operator on a computer, the filter must run with $2N$ significant figure arithmetic to be sure of obtaining an N significant figure result. [7]

Different types of estimation problems may require different estimation methods based on the size of the data given and state. The method of least squares requires an inversion of the covariance matrix, which is of the order of the state vector, whereas

the Kalman filter rearranges the method of least squares in a way that only requires an inversion of a matrix the order of the data vector. Because of this, when processing a large state vector with little data, the Kalman filter is a favorable approach. On the other hand, when processing large amounts of data in one update, the method of least squares is a more efficient estimation approach. The Kalman filter may run into problem in orbital estimation problems when perturbations such as air drag are present. Because air drag's effects are felt over long periods of time, using methods that only use a short amount of data over a short amount of time will not take these effects into consideration. In order to make an accurate estimate, sequential operators such as the Kalman filter must be fed a large enough amount of data that is capable of observing the effects of air drag. [7] A Kalman filter was used in SOS's GPS receiver in order to propagate position estimates. However, errors in the navigation solution were encountered with the absence of new navigation data. [12] The method of iterative least squares was applied in both the SOS SGP4 OD algorithm and the SP OD algorithm being analyzed for this thesis research.

2.2.3 Propagation Methods

The growing use of computers has increased the ability to propagate orbits more accurately. However, before such computing power was available, other propagation methods were necessary. Depending on the computing power available to a system, propagators will either use numerical integration or approximate series solutions to the equations of motion, known as special perturbation and general perturbations, respectively. [7] North American Aerospace Defense Command (NORAD) classifies all space objects as either near-Earth, which have an orbital period less than 225 minutes, or deep-space, which have an orbital period greater than or equal to 225 minutes. A propagation model is chosen depending on this classification. [36]

The general perturbations method uses the approximate series solutions to the equations of motion to give the osculating orbital elements as a function of time. This set of orbital elements is then used in the two body problem to determine the actual position of the satellite. This method has fast execution time but is limited in solution complexity and limitations to small eccentricity. The general perturbations method mostly models the dynamics on a satellite caused by the gravitational effects of the Earth and air drag. [7]

The SGP4 propagation model is an analytical method used for generating ephemerides for satellites in Earth-centered orbits based on general perturbation theory and uses an iterative least squares approach to complete estimation. [37] It was developed by Ken Crawford in 1970 and is used for near-Earth satellites. This model uses the solution developed by Brouwer for its gravitational model and a power density function for its atmospheric model, obtained from a simplification of the more extensive analytical theory of Lane and Cranford. [36] Due to the limited computing capacity at the time of SPG4's development, modifications to the general perturbations solutions had to be made. Simplifications to the gravitational model were made by including only long and short periodic terms that do not include eccentricity as a factor. Also, only the main terms that modeled the secular effect of air drag terms were included. [26] This method is what the JSpOC currently uses for propagating their TLEs, although there has never been a release of any kind of differential correction code to implement the SGP4 method due to the code being proprietary. [37, 38] In 2006, David Vallado published a version of SGP4 for general use capable of using TLEs as input to create an orbit prediction in C++. [38] An adapted version of this code using an iterative least squares routine was used as an orbit determination method on SOS implemented in C code. However, the typical accuracy of the algorithm found on-board SOS was approximately ten kilometers at epoch, with SGP4 increasing the error by an average

of two kilometers per day. [12]

The method of special perturbations, also known as precise orbit determination, has become more common as the space industry moved out of the era of expensive, large mainframe computers. Special perturbations programs are relatively easy to write and can handle any type of orbit. In order to use special perturbations approach, the equations of motion of the two body problem and equations of variation are numerically integrated using the inertial position of the satellite given either through ground based or space based tracking techniques. For high precision work, small corrections to the Earth's precession, nutation, and Chandler wobble are taken into account. The dynamics in the two body problem include any other forces that the satellite might encounter, not just air drag and gravitational forces. [7] Because an accurate dynamics model is crucial to modeling perturbing forces necessary to complete precise orbit determination, extensive research has been conducted in order to improve the models. As a result of this work, a comprehensive set of force models have been developed including gravitational models. [39] Currently, satellite orbits determined through the use of special perturbations techniques have displayed centimeter level accuracy. [40] Although SOS currently uses SGP4 for orbit determination, a special perturbations approach can be tested as an alternative method in order to improve the accuracy of the orbit determination data. The possibilities for further improvement to special perturbations remain possible as dynamics models continue to be refined.

2.3 Time Standards

Using standardized units in calculations and measurements has always been an integral part of any engineering problem. Time measurements, specifically, have created challenges as standards can differ from user to user. This section describes

the history and variety of standards of time measurement of which the two main types are rotation and atomic based. These standards are discussed as well as the systems of time measurement that lie within each category. The difficulties encountered while using certain time scales, specifically with leap seconds, are also presented.

2.3.1 Rotation and Dynamical Based Systems

The diurnal changes in the environment of the Earth, or the motion of the rotating Earth with respect to the stars, provide an obvious choice for the measurement of time. Using celestial observations, astronomers have developed several series of timescales that measure time either from the motion of the Sun or stars, such as the timescales described in the subsections below. [41] With the approach of the twentieth century, inaccuracies were found within rotation based timescales which required a more uniform timescale that is not based on the dynamic motions of solar system bodies.

2.3.1.1 Solar Time and Sidereal Time

Rotation based timescales can be measured with respect to either the Sun or stars as a reference. The measurement of the Sun's hour angle is defined as "apparent solar time". This approach depends on the location of the observer on the Earth and allows for variations in the duration of each apparent solar day depending on the day of year since the Earth's orbit is not circular and is inclined with respect to Earth's equator. In order to address these variations, a new form of time measurement was developed called "mean solar time". Mean solar time uses an artificial point called the "mean sun" that moves uniformly along the plane of the Earth's equator at a rate equal to the average rate of the Sun in the ecliptic, or the apparent annual path of the Sun against the background of the stars. [41, 42] Another form of time measurement based on

rotation rates is "sidereal time". Sidereal time is defined as the rotation of the Earth with respect to the stars and depends on the location of the observer. Because of the precession of the Earth's axis with respect to the celestial reference system, a sidereal day is 0.0084 seconds shorter than actual period of rotation of the Earth in inertial space. [42] Several more standards of time measurement were established based on the Greenwich meridian such as Greenwich Mean Time (GMT) and the emission of time signals by radio stations known as Greenwich Civil Time (GCT). Even these scales varied by what time they were originally established, either noon to noon or midnight to midnight. Because so many different standards of time measurement existed, the International Astronomical Union (IAU) recommended using the name "Universal Time" to replace both GMT and GCT in 1928 [41].

2.3.1.2 Universal Time

Universal Time (UT) is the measure of astronomical time defined by the rotation of the Earth on its axis with respect to the Sun (i.e. the diurnal motion of the Sun). It is essentially the same as mean solar time, except it is exclusively measured from the Greenwich meridian and is measured from midnight to midnight. Also, unlike mean solar time, UT is determined specifically by the diurnal motion of the vernal equinox, which is the intersection of the ecliptic with the celestial equator, instead of the meridian transit of the mean Sun. [42]

There are three recognized versions of universal time by the IAU: UT0, UT1, and UT2. The Greenwich mean solar time observed from any location on the Earth is defined as UT0. Because of its neglect of the variation of latitude, the torque-free precessional motion of the Earth's axis of rotation with respect to the Earth's surface, UT0 is no longer in common use. Taking this into consideration, UT1 was established from UT0. While accounting for the variation of latitude, UT1 differs from UT0 at a

maximum of about 20 milliseconds at mean latitude. [42] The final form of universal time, UT2, is derived from UT1 and accounts for the observed seasonal variation in the Earth's rotational speed shown in Eq. (7), where t_b is the fraction of the Besselian year and units are seconds. [41]

$$UT2 = UT1 + 0.022 \sin 2\pi t_b - 0.012 \cos 2\pi t_b - 0.006 \sin 4\pi t_b + 0.007 \sin 4\pi t_b \qquad (7)$$

The rotation of the Earth runs about 30 milliseconds fast in November and slow in May, causing a seasonal variation of the length of day on the order of 0.5 milliseconds about the mean. [42]

2.3.1.3 Ephemeris Time

Due to the variety of time scale definitions that depend on the complex rotation of the Earth, a more uniform measurement of time, independent from the rotation of the Earth, was needed in the astronomical community. As a result, "ephemeris time" was developed in the 1950s. Ephemeris time is based on the period of the revolution of the Earth around the Sun assuming Newtonian mechanics, published in Newcomb's Tables of the Sun in 1895. [42] Initially, the revolution period of the Earth was based off the length of a sidereal year (fixed star to fixed star), which depended on the value of precession. [42] However, Andr Danjon determined that the period of revolution is actually the length of a tropical year, or the interval during which the Sun's mean longitude (mean equinox of date) increases by 360 degrees. [42, 43] Therefore, IAU General Assembly defined the epoch of ET by: "Ephemeris Time (ET), or Temps des Ephemerides (TE), is reckoned from the instant, near the beginning of the calendar year A.D. 1900, when the geometric mean longitude of the Sun was $279°41'48.04''$, at which instant the measure of Ephemeris Time was 1900 January 0d 12h precisely," and was defined from Newcomb's expression. [41] The date 1900 January 0d 12h is

referred to as the "fundamental epoch." [43] In practice however, ephemeris time was found using observations of the position of the Moon with respect to the celestial reference frame and was determined by Eq. (8) , where T was determined from these observations and could be found in *The Astronomical Almanac*. [41]

$$ET = UT1 + \Delta T \tag{8}$$

Although ET replaced UT as the independent variable of astronomical ephemerides, it still does not account for relativistic effects and was inconvenient to obtain in real-time. [41] This lead to the formation of atomic based time scales, discussed in the next section.

2.3.2 Atomic Based Systems

Rather than relying on astronomical repeatable events to mark the passage of time, physicists started pursuing a more uniform timescale using molecular and atomic clocks. This technology uses the energy level transitions in alkali elements to produce a stable frequency to drive the clocks. [41] Around the same time that ephemeris time was being established in the 1950s, Essen and Parry of the National Physical Laboratory in the United Kingdom were working to measure the operational frequency of the laboratory's caesium standard to the second of UT2. They accomplished this by the comparison of the adopted frequency of a quartz standard that was calibrated from astronomical measurements. Later, the team was able to calibrate the frequency in terms of the Ephemeris Time second using dual-rate Moon camera observations to determine Ephemeris Time from a position of the Moon at a known UT2 over the period of 1955.50 to 1958.25 in conjunction with the United States Naval Observatory. The caesium frequency measured was 9,192,631,770 Hz with a probable error of $\pm$ 20 Hz due to the uncertainty of the measurement of ET. [41,42] From this mea-

surement, the atomic second was adopted as the new fundamental unit of time in the International System (SI) of Units and was defined as "the duration of 9,192,631,770 periods of the radiation corresponding to the transition between the two hyperfine levels of the ground state of the caesium 133 atom." [42] This definition of the second is in principle equivalent to the ET second and also approximately equal to the mean value of the UT1 second in the 19th century. [41] From the development of the atomic second, many different atomic time scales were developed across laboratories and institutions. In order to meet the desires of those who wanted time to be derived from the Earth's rotation in space and those who wanted time to be perfectly uniform with the best atomic clocks, a new time scale was created called "Coordinated Universal Time." [42]

2.3.2.1 Coordinated Universal Time

Coordinated Universal Time (UTC) was defined by the need of a universal time scale among the countries of the world. Before its creation, time signals broadcasted from various countries were so loosely controlled that their transmissions would all arrive at different times. Because of this, a worldwide scale was needed. With the combination of the United Kingdom and United States nautical almanacs and time and frequency transmissions in 1960, other countries began to join the system. By 1967, UTC was approved. [42]

Originally, UTC was defined yearly to match the rotational speed of the Earth by the insertion of 100 millisecond time steps as needed at the beginning of each month in order to maintain time that was within less than 0.1 seconds of UT2. Because UTC included these offsets, the broadcasted time signals were neither the SI second nor the mean solar second. [42] The variability of these time transmissions resulted in the frequent adjustments to complex electronic instrumentation. [41] It was suggested

that the UTC rate offsets and step adjustments be discontinued and that the SI definition of a second should be used. [42]

In order to remain within a reasonable tolerance of UT but discontinue the use of rate offsets and step adjustments, the concept of a leap second was introduced by Winkler and Essen. [42] By using a 1 second step adjustment (insertion or deletion) without offset rates, adjustments would no longer require a frequency change. In 1973, the recommendation of the leap second was formalized and the defined UTC system to act as a basis of standard time in all countries. The leap second was defined in a way that the limit of [UT1-UTC] was set at $\pm$ 0.95 seconds, which is the maximum difference that can be tolerated by code format, with a tolerance of 0.7 to 0.9 seconds. The maximum deviation of UT1 from [UTC + DUT1] was set at $\pm$ 0.100 seconds, where DUT1 is the difference between UT1 and UTC. [42] The preferred times to either subtract or add a leap second are at the last minute of June 30 or December 31 or, as a secondary choice, March 31 or September 30. [41] This definition of UTC is still in practice today, although it remains a topic of controversy.

2.3.2.2 Leap Seconds

Leap seconds are added in order to account for the Earth's rotation running slower than atomic time. Because the mean solar day was measured at 86,400 seconds (the length of a day in SI units), the length of the day has increased by 2.5 milliseconds over the past 180 years. This increase in day length has resulted in about a 1 second increase over an entire year, which is the reason for the insertion of leap seconds. [42] Since the establishment of UTC as the standard for civil timekeeping, there has been 26 leap seconds added, resulting in UTC being behind International Atomic time by 36 seconds. The most recent addition of a leap second was added on June 30, 2015 at 23:59:60 UTC. [44]

Some would prefer that the use of leap seconds would be discontinued, which will be discussed further in the next section. Many people within the space community, such as astronomers and satellite ground-station operators would prefer that leap seconds not be eliminated, however, because of the legacy software they use that requires that DUT1 should always be less than 1 second. Other areas that would be affected by the loss of leap seconds are the transmission formats for radio and telephone broadcasts of time signals and clocks in the commercial industry that receive radio broadcast time signals to display accurate time automatically. [42]

2.3.2.3 Difficulties with Leap Seconds

Many issues arise with the implementation of leap seconds. Many systems rely on precise time synchronization and may become corrupt during the introduction of a leap second. Systems such as telecommunication systems can lose communication until synchronization has been re-established. Another complication with leap seconds comes from the extensive use of time in today's computer systems. Because computers usually run on a count sequence that goes from 59 to 0 seconds, the increase to 60 seconds produces a problem.

Another concern is with the use of Julian Days (JD) or Modified Julian Days (MJD). The Julian Date is the number of days that has elapsed since January 1, 4713 B.C. at Greenwich noon on the day designated, followed by the fraction of the day elapsed since the preceding noon. [43] The Modified Julian Day was introduced in the late 1950s and is shown in Eq. (9).

$$MJD = JD - 2400000.5 \tag{9}$$

In order to keep the MJD in accordance with civil time, the half day was subtracted so that the day starts at midnight instead of noon. This system of time is a convenient

dating system with only 5 digits. [45] The problem when using JD or MJD is that when a leap second arises, it would create a situation where two events 1 second apart can receive identical dates when they are expressed with a numerical precision equal to 1 second. [42]

GPS uses its own system of time, called GPS time. This time scale is a continuous time count with no discontinuities, from the GPS epoch of January 6, 1980 at 0 hours (midnight) UTC. It is based off UTC time, but does not account for leap seconds. GPS time is formatted by weeks and seconds of a week from the GPS epoch. The week begins at the transition from Saturday to Sunday. Both the days of the week and the week number begin at 0. [46] The GPS Week Number rolls over after 1024 weeks, meaning that at the completion of week 1023, the GPS week number changed to 0 at midnight GPS Time. This occurred on August 21, 1999 at 23:59:47 UTC. The next GPS week number rollover will occur in April 2019. [47] It is specified to be within 1 microsecond of UTC but without inserted leap seconds, with Eq. 10 demonstrating the relationship between GPS Time and UTC. [48]

$$\text{GPS Time} = \text{UTC time} + (\text{number of leap seconds} + \text{GPS to UTC bias}) \tag{10}$$

As of August 2015, GPS Time is ahead of UTC by seventeen seconds. [49] Both the GPS week number rollover and the absence of leap seconds can cause issues for users of GPS time. It is the responsibility of the user to account for the previous 1024 weeks if a rollover has occurred and to make sure that systems using multiple systems of time are accounting for leap seconds.

When performing operations that involve differing hardware and software systems based on varied standards and practices, the introduction of leap seconds could directly affect synchronization. [42] This problem was directly encountered in the previous work accomplished on the SOS system by Jenson. It was found that dis-

crepancies in the data were caused by the use of GPS time and converting this time to the Julian date in UTC time. [12] Instances such as this are very common as real-world operations are confronted by equipment upgrades, system integration, and personnel changes. [42] In order to minimize the risk of problems with leap second synchronization, either non-traditional systems of timekeeping are being implemented, such as GPS Time, or careful consideration must be made in regards to time measurement.

2.4 Relevant Efforts

The topics discussed in this thesis have had a significant amount of research previously performed. Prior to this thesis, efforts from six other AFIT students have been put toward the SOS mission and are described in this section. The relevant efforts towards the topic of GPS-based orbit determination are also discussed.

2.4.1 Previous SOS Research

A significant amount of research efforts by AFIT professors, staff, students, and interns has been put forth to ensure success on the SOS mission. [12–14, 50–52] Previous research has focused on supporting payload verification and validation activities, as well as specifically focusing on evaluating the on-board SGP4 OD algorithm performance. Since 2013, there have been several theses focused on research related to SOS.

Claybrook [50] investigated the feasibility of RSOs in LEO communicating continuously with the ground through the use of the Iridium SATCOM Network and found that Iridium provides significantly more communication opportunities in comparison to ground-based communications using a single ground station. Bastow [14] created the PACS system architecture and studied the impact of the accuracy of conjunction analysis performed by JSpOC when RSOs are equipped with PACS. The results of

Bastow's thesis showed that PACS can significantly improve the accuracy of conjunction analysis and found that PACS provided the biggest impact on non-active RSOs since their initial uncertainty is much larger than active RSOs. Newman [51] examined methods of analysis and validation for solar arrays and batteries in the context of the SOS design and found that body mounted solar arrays provided the best results during worst-case power generation conditions.

Hardware analysis and environmental testing of SOS was performed by Perry. [52] TVAC testing was performed, as well as the analysis of existing SOS hardware's ability to meet requirements, finite element analysis (FEA) and verification of the SOS chassis, and trade space analysis of chassis and board stack configurations. Through Perry's research efforts, it was found that the chassis and internal components met the structural requirements for the launch environment. Schaffer [13] investigated the use of the Iridium constellation as a means for SOS to transmit precision tracking and identification information to the ground user, specifically studying the effects of altitude, antenna pointing, Doppler shift, and link margin on the SOS communication link with Iridium. The results of Schaffer's research showed that SOS's access with Iridium increased with decreased altitude, the use of targeted pointing is not required, and the link margin between SOS and Iridium was viable at all potential ranges that will be encountered during the SOS experiment.

The sensitivity of GPS positioning and the OD algorithm performance to attitude, orbit, data sampling rates, and duration was studied by Jenson [12]. Through this research, it was found that SOS should receive nearly uninterrupted GPS service in both the zenith- and velocity-facing orientations at all tested altitudes and inclinations; however, the zenith-facing orientation was recommended as the primary operating attitude. Using SGP4 as the OD algorithm for SOS, Jenson found that a propagation error of around 2 kilometers per day was exhibited with a recommended

sampling rate of one sample every minute for 24 hours. Overall, Jenson's results validated GPS access and positioning accuracy for SOS.

2.4.2 Previous Efforts Related to GPS Based Orbit Determination

With the introduction of space rated GPS receivers, today's satellites carry the ability to achieve high accuracy orbital predictions through the use of almost continuous tracking data. Several missions have used this capability to process orbit predictions both on the ground and autonomously on-board the spacecraft using different types of prediction algorithms. [39, 53–60]

Most precise orbit determination (POD) is done on the ground in postflight mode. [53] The ground-based processing of raw GPS pseudorange data using POD for the following missions was and is currently still performed using the NASA Jet Propulsion Laboratory (JPL) GNSS-Inferred Positioning System and Orbit Analysis Simulation Software (GIPSY OASIS II) software Package. [39, 54, 55] The TOPEX (Topography Experiment)/Poseidon (T/P) mission, conducted by NASA and the French Space Agency, Centre National d-Etudes Spatiales (CNES) was conducted to improve the knowledge of global ocean circulation. The T/P spacecraft is at an orbit of 1336 kilometers, 66 degree inclination, and a near-zero eccentricity. Because of a stringent accuracy requirement, the satellite's orbit must be predicted no greater than an RMS radial accuracy of 13 centimeters. In order to achieve this accuracy, the T/P satellite is equipped with a GPS receiver that can track up to six GPS satellites at once in both frequencies if antispoofing is inactive. [56] Radial accuracies for T/P have been demonstrated to be about two to three centimeters RMS. Accuracies of this level were able to be achieved due to the high altitude of T/P which provided smaller errors from geopotential and atmospheric drag perturbations. [39]

The successor to the T/P mission, Jason-1, lies in the same orbit as T/P with

the same mission. However, it has been able to reach RMS radial accuracies of better than 2 centimeters. [56] The GRACE mission, already discussed in Section 2.1.2.2, launched in 2002 and used GPS measurements calculated from a BlackJack GPS onboard receiver to continuously and accurately determine the orbits of its spacecrafts. Using this technology, orbits have been estimated using ground-based precise orbit determination methods to a degree of 5 centimeters in each direction. [56] Another satellite used for geophysical research is the CHAllenging Minisatellite Payload (CHAMP) German small satellite launched in July 2000 in a near polar orbit of about 454 kilometers. [57] CHAMP's mission was to resolve long-term temporal variations primarily in the magnetic field, gravity field, and within the atmosphere. Using GPS navigation data provided by a BlackJack GPS receiver, CHAMP was able to achieve a position accuracy of about 0.8 meters. [56, 57] The use of precise orbit determination of low earth satellites using GPS navigation solutions has continued to grow over the years and includes more satellites than those listed in this thesis.

Using GPS navigation data to autonomously conduct orbit determination onboard a spacecraft is less common. However, current technology is making this practice a more conceivable possibility for future spacecrafts. [53] NASA's Goddard Space Flight Center (GSFC) has created the GPS-Enhanced Onboard Navigation System (GEONS) which processes data from standard GPS receivers, onboard communication equipment, and/or attitude sensors to produce accurate navigation solutions in real time with fewer than four visible GPS space vehicles. This software uses an extended Kalman Filter to calculate a state estimation and state error covariance to estimate a spacecraft's orbit and can work autonomously on an onboard computer. State estimates are even able to be generated during complete GPS coverage outages. GEONS has been able to achieve accuracies of at least 20 meters for position estimates and three centimeters per second for velocity estimates. [58] Although GEONS

is highly beneficial, it is not able to achieve the amount of accuracy found through POD.

Another example of onboard orbit determination is the Thermosphere, Ionosphere, Mesosphere Energetics and Dynamics (TIMED) spacecraft, designed as the first Solar Terrestrial Probe in NASA's Solar Connections Program. TIMED was launched on 7 December 2001 to a circular orbit at an altitude of 625 kilometers with an inclination of 74.1 degrees. The TIMED GPS Navigation System (GNS), uses its GPS receiver and orbit propagator for onboard tracking, navigation, and event-based commanding. Utilizing the a single-frequency Standard Positioning Service GPS receiver, TIMED is able to determine its position to less than 300 meters and velocity to 25 centimeters per second. [59] Using this GPS navigation data, a Kalman filter orbit estimator extrapolates the spacecraft orbits for 24 hours, updating on an hourly basis. [59, 60]

Although several systems exist similar to the concept of operations of SOS and the research conducted in this research, their philosophies differ in their method of producing orbit estimates through the use of the pseudorange and pseudorange rate evaluated by the GPS receiver instead of the calculated GPS navigation solution. While there has been many cases of the use of POD (very similar to the SP algorithm used for this research) using GPS data, the similar missions do not use this method when processing orbit estimates onboard the spacecraft.

3. Methodology

This chapter describes the methods used to collect and analyze data in support of the research objectives described in Section 1.3. The experimental design of this research is first discussed, followed by a summarization of the SP algorithm used for this thesis by describing the SP code specifically, the integrator and dynamics model used, and the different types of truth data used as input for the code. Next, through discussion on the SP algorithm development, the validation of inertial position and GPS sentence input data and the truth model is presented. This chapter concludes by describing the implementation of experiments and analysis completed on the SP algorithm.

3.1 Experiment Design

As discussed in Chapter 1, the focus of this research is to investigate the modification of an existing SP orbit determination algorithm and analyze the effects of using GPS NMEA sentences as input to the accuracy of the algorithm. The SP algorithm tested for this research could either be used to further ground-based processing of the raw GPS data received from SOS or could possibly replace the existing SGP4 OD algorithm currently in use for flight on SOS. Specifically, this research focuses on modifying an existing piece of SP algorithm written in C++ code developed by an AFIT faculty member, Dr. William E. Wiesel, which previously only received input data in the form of time and inertial position vectors. In order for data to be processed from SOS, the SP code had to be enhanced to take in GPS data as input and convert it to an inertial position and time for propagation. After developing and modifying the SP algorithm, the accuracy of orbit predictions are validated, analyzed, and compared to the results of the current SGP4 OD algorithm. The accuracy results

can also be used to determine if SP is a viable option for processing data received by SOS's GPS receiver to determine orbit predictions.

In order to create "truth" data for accuracy comparison of the orbit predictions, an orbit similar to one expected on SOS's upcoming mission was modeled and simulated in STK originally using the J4 propagator, then redone using STK's HPOP, including perturbations due to Earth's geopotential effects to twentieth order. The orbit scenario for this experiment was chosen by using the same scenario used for previous analysis of SGP4 performed by Jenson [12], shown in Table 4. Using the SOS simulation provided by Jenson, STK determined an orbit trajectory in the form of time, inertial position, and inertial velocity. The scenario trajectory propagated STK was then converted to GPS sentences in order to simulate what the SOS OD algorithm would receive from the SOS OEM615 GPS receiver. The STK input to GPS sentence conversion was applied using both a GPS signal simulator and a conversion algorithm written by Dr. Wiesel.

Table 4. SP Simulated Orbital Scenario

Simulation	Altitude	Inclination	RAAN	True Anomaly	Arg. of Perigee	Eccentricity
SOS3z	625 km	24.5°	0°	0°	0°	0

The SP algorithm provided for this research uses observational and state data and a dynamics model to propagate an orbit trajectory forward in time. The format for the observation and state data used in the SP algorithm was originally written with positions and velocities in the inertial frame. Because SOS is fitted with a Novatel OEM615 GPS receiver, SOS produces its position data in the format of GPS National Marine Electronics Association (NMEA) sentences. Two types of NMEA sentences are used for observation data in the SP algorithm, GPGGA and GPZDA. The GPGGA sentence contains UTC time, position in latitude, longitude and altitude, and other performance metrics such as dilution of precision and number of

satellites in use. In GPZDA format, the UTC time and date are given. [61] The modified SP algorithm instead uses GPS NMEA sentences as input and converts the data into the inertial frame for processing. More information on the GPS sentence to inertial position conversion algorithm is discussed later in this chapter. The SP algorithm then numerically integrates calculated equations of motion (EOM) and the equations of variation (EOV) using the inertial position of the satellite. The EOM are developed from a dynamics model, which takes into account the perturbations that can change the orbital trajectory as a function of time. Types of perturbations that a satellite may face include air drag, third body motion due to objects such as the moon or sun, and variations in the gravity of Earth. Once the EOMs are found, the new orbital trajectory can be determined through the method of iterative least squares. More information on the OD processes used for this thesis is found in Section 2.2.

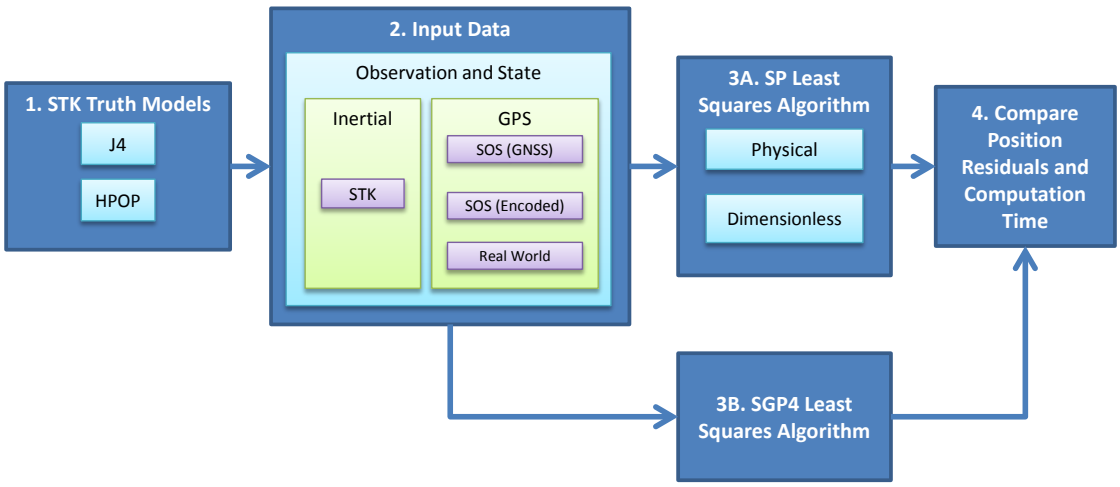

Figure 12. SP Algorithm Validation Process

The process used to validate and test the modified SP algorithm is depicted in a block diagram shown in Figure 12. This diagram describes the variations tested in STK truth models, input formats, versions of the SP algorithm, and the final output. One of the important first steps in this research is to validate the modified

SP algorithm. The truth model created by simulating the SOS orbit in STK also had to be propagated forward in time in order to provide comparative results. The options for propagators within STK depends on the perturbations applied to the spacecraft. The propagation methods used for this research included J4, which was used for analysis on the SGP4 algorithm, and HPOP. J4 generates the solution for the vehicle moving about a central body considering the effect of the body viewed as a point mass, or the solution to the Two-Body problem, as well as the dominant effect of the variations in the gravitational field of the Earth due to the Earth's oblateness. J4 describes the zonal coefficients that depend on latitude. [62,63] On the other hand, HPOP uses numerical integration of the differential equations of motions to generate ephemeris data for the space vehicle. The force models included in HPOP can include a full gravitational model up to the user's specified zonal harmonic, third-body gravity, atmospheric drag, and solar radiation pressure, but was set to only includes Earth's geopotential effects for this research. HPOP uses techniques very similar to those used in SP and provides a much more accurate trajectory. [64]

Once the "correct" truth data was computed, the different types of allowable input data shown in the second block in Figure 12 in both inertial and GPS sentence format, were tested to provide validation. Each input format data set was derived using the same orbit simulated in STK. Validation of the modified SP algorithm including the addition of the GPS input format required careful consideration. In particular, validation of the state corrections through singular value decomposition brought out issues with the use of physical units and the algorithms ability to process the information using double precision computation. These errors required the SP algorithm to be converted from physical units to dimensionless units, which were based upon the radius of the Earth and the standard gravitational parameter of the Earth μ. Each of the input data types found in the second block of Figure 12 was used

to test both the physical and dimensionless unit versions of the algorithm, represented in the third block of Figure 12. In each of the test cases, the orbital trajectory was propagated in the SP algorithm and compared to the original reference trajectories to find the OD algorithm's accuracy, represented by position residuals. The overall accuracy found from SP was used to characterize the impact of using GPS data on SP and compare the results to those found from previous SGP4 analysis provided by Jenson [12].

3.2 Special Perturbations Least Squares algorithm Overview

The algorithm being evaluated in this thesis implements an SP orbit determination process that numerically integrates the EOM and EOV of an object in space and propagates the state, in the form of an inertial position and velocity vector, forward in time. To achieve these results, an SP least squares method, dynamics model, GPS to inertial conversion, and hamming integrator are used throughout the overall algorithm package. For this thesis, the manipulation and testing specifically focused on the SP least squares algorithm. Figure 13 represents a pictorial representation of the flow of the SP least squares algorithm.

There are two requirements for the SP algorithm to estimate an orbit, observation data of the spacecraft and a dynamics model. The observation data to be processed through this algorithm needs to be in the inertial reference frame. Therefore, the SOS GPS NMEA sentences must be converted to an inertial position vector upon input (Figure 13 Block 3B.1). An initial state of the spacecraft, including the epoch time, inertial position vector, and inertial velocity vector, is also required to determine the spacecraft's final estimated state. Depending on the what method of observation data input is used, the initial state is found in different ways. If the initial input was in the form of inertial data, the state is provided through input that includes the first entry

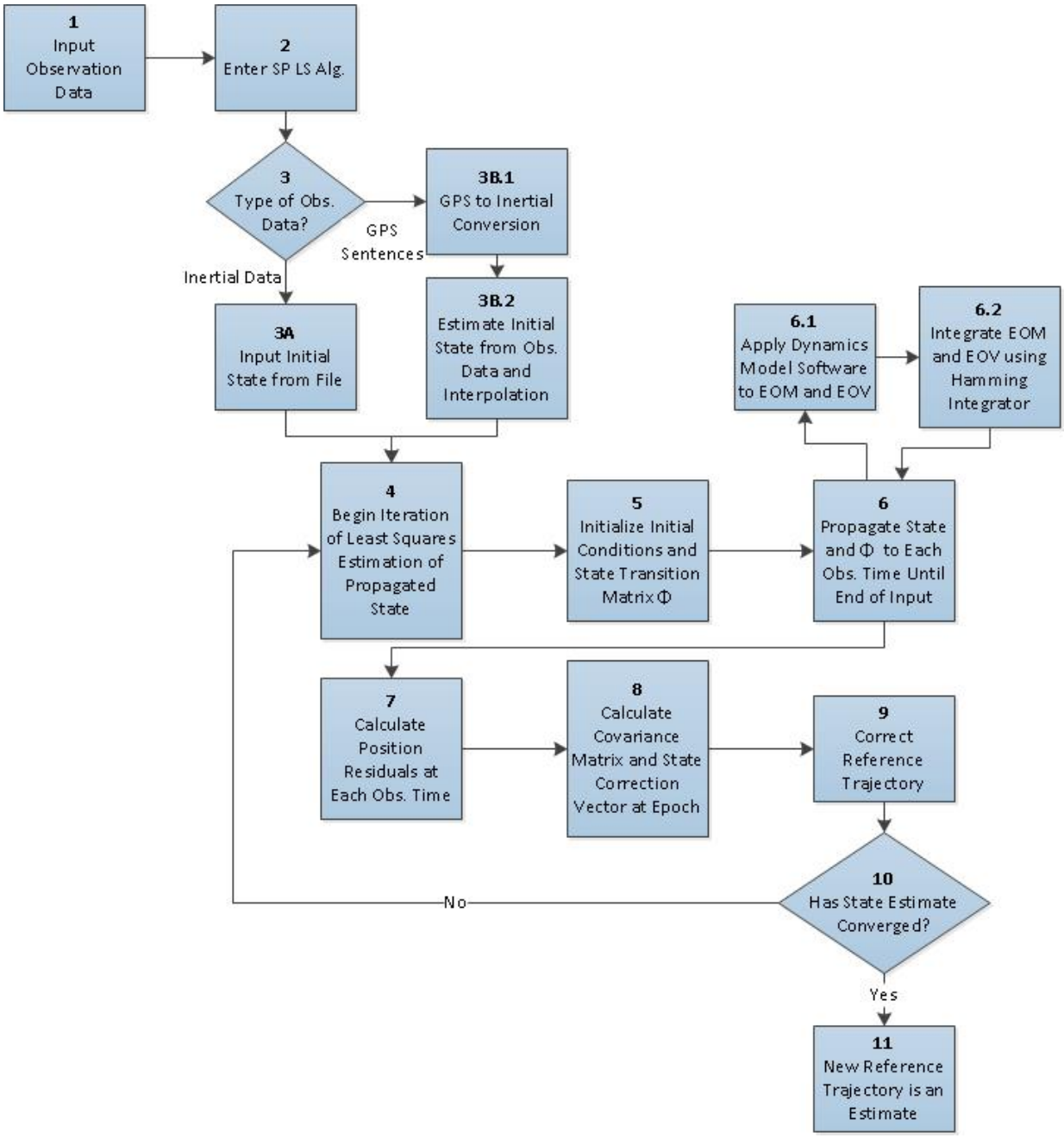

Figure 13. SP Algorithm Flow

of observed position, velocity, and air drag coefficient (Figure 13 Block 3A). However, if the observed data came in the form of GPS sentences, only the initial position and time of epoch are known for the spacecraft's state. Using the first three position data entries, a Lagrange interpolation derivative evaluated at the epoch time is used to find a the velocity of the spacecraft for the initial state (Figure 13 Block 3B.2).

Once the initial state and observation data are determined for the spacecraft, the algorithm enters a least squares estimation loop (Figure 13 Block 4). The initial conditions, or the initial state, and the state transition matrix Φ, which is the derivative of the state solution at a given time with respect to the initial conditions, are first initialized to start the least squares process (Figure 13 Block 5). Next, the least squares algorithm propagates the state vector and Φ matrix to each observation time. Propagation is completed outside of the least squares algorithm by calling upon a dynamics model and integrator. Through the dynamics model, perturbations are included in the calculation of both the EOM and EOV, which model how the state changes over time and how the original reference trajectory changes with respect to a change in the initial conditions (or how it changes by applying perturbations to the system), respectively. The EOM and EOV are determined through the application of Hamiltonian equations, the Two-Body Problem, and applied dynamics (Figure 13 Block 6.1). Once the EOM and EOV are determined, they are numerically integrated within the dynamics model to provide a new state and state transition matrix Φ at a given observation time using a Hamming integrator (Figure 13 Block 6.2).

In parallel to the integration process, the new state data is compared to the observation data at the same observation time through the calculation of residuals outside of the dynamics model (Figure 13 Block 6-7). After the change between the state and observation at each observation time is calculated, a covariance matrix and state correction are calculated at the epoch time to be applied to correct the

reference trajectory (Figure 13 Block 8-9). The least squares algorithm compares the new reference trajectory to the previous one and determines if convergence has been found in the estimate (Figure 13 Block 10). If the solution has not converged, the least squares method is applied through iterations by rerunning through Blocks 4 through 10 in Figure 13 until convergence has been determined. Once convergence has been signaled within the algorithm by reaching a set convergence limit, the new reference trajectory, which now includes dynamics applied to the initial state, is labeled as the state estimate for the spacecraft (Figure 13 Block 11). More information on least squares, propagation methods, and perturbations can be found in Section 2.2. A more detailed explanation of SP least squares supporting algorithm is discussed in the following sections.

3.2.1 GPS to Inertial Position Conversion

Because the observation data provided from SOS is written in terms of NMEA sentences, it is necessary to convert the data into the inertial frame. This process was completed within the SP Least Squares algorithm through a separate conversion process provided by Dr. Wiesel. The algorithm is written to convert the two types of NMEA sentences expected from SOS, GPGGA and GPZDA. As GPZDA only provides a date and time in UTC, the algorithm parses out the input data and uses the date and time to convert the data to a Julian Day number.

Processing the GPGGA data is a more complicated process. First, if the Julian day number has not yet been calculated through the GPZDA sentence, the time information, given in UTC, is converted to a Julian Day. The position of the spacecraft is provided in terms of geodetic latitude and longitude in degrees which is described in Figure 14. In order to calculate an inertial position vector, the latitude must be converted from geodetic to geocentric. Geodetic latitude measures the angle between

the equatorial plane and the line coming from the spacecraft to the plane normal to the ellipsoid of the Earth. Geocentric latitude, on the other hand, measures the angle between the equatorial plane and the line coming from the spacecraft to the center of the ellipsoid of the Earth. Once the latitude is converted to geocentric, the position data in the latitude, longitude, and altitude (LLA) coordinate frame is converted to a position vector in the Earth-centered Earth Fixed (ECEF) frame, a Cartesian reference frame that rotates with the Earth in order to remain fixed with respect to the surface of the Earth. The altitude used in this conversion is found from the antenna altitude and the geoid height collected by the GPS receiver and is converted from meters to kilometers. Once the data is in the ECEF frame, it can be converted to the Earth-centered Inertial (ECI) frame, which is a Cartesian frame whose origin is at the center of mass of the Earth and is fixed in inertial space. The conversion from ECEF to ECI uses Greenwich sidereal time in radians as the angle of coordinate transformation, which measures the hour angle of the vernal equinox. A correction was also made to the inertial positions to take into account precession effects using the J2000 epoch, or the equinox and mean equator of 1 January 2000 at 12:00 UT. [65] Descriptions of each coordinate system used in the conversion from GPS sentences to the inertial frame are shown in Figure 14. [34, 66]

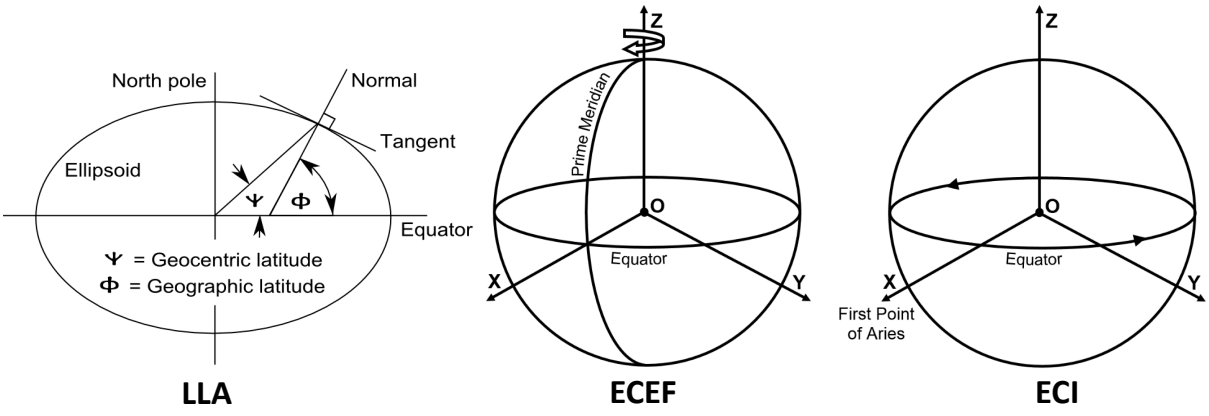

Figure 14. Coordinate Frames Used in SP Software [34, 66]

3.2.2 Dynamics Model

The dynamics model is used to calculate the EOM and EOV of the system. Perturbations are applied to the system to provide the most accurate estimate for the equations and to show how the initial state will change over time due to outside forces. The dynamics model used for this research included the perturbations applied to the system through the Earth's geopotential. However, the capability to include perturbations caused by air drag and the third body effects of the Moon and Sun are also included in the model but not enabled in this research. The model reads in the EGM96 geopotential model, which is a spherical harmonic model of the Earth's gravitational potential complete to the degree and order of 360. The order used in the algorithm is specified through the input data, and is set to order 20, but can go as high as 50. The model may work in either the ECI or ECEF frames, but for this research, the ECI frame was chosen. The model also allows for calculations to be completed in either physical or dimensionless units based on the Earth's radius and the standard gravitational parameter of the Earth μ. For this research, both options were analyzed.

A Hamiltonian equation, which models the dynamics of the system, is found using the geopotential model to the order specified and adding any other additional perturbations felt by the system. For this research, the Hamiltonian included the kinetic energy determined from the Two Body Problem and the geopotential expansion up to order 20, shown in Eq. (11) where H is the Hamiltonian or the kinetic energy T plus the potential energy V, x, y, z are the inertial position vector components of the spacecraft, p_x, p_y, p_z are the generalized momenta, and $V(x,y,z)$ is the geopotential expansion function. The EOM $\vec{f}$ are calculated by taking the partial derivative of the Hamiltonian with respect to each component of the state $\vec{x}$, shown in Eq. (12) where $\frac{\partial V}{\partial x}, \frac{\partial V}{\partial y}, \frac{\partial V}{\partial z}$ are the partials of the geopotential with respect to either x, y, or z.

Using the calculated EOM, the EOV in Eq. (13) are found by calculating the change in the state due to a change in the initial conditions of the state (Φ matrix), as well as calculating the change in the EOM due to a change in the state (A matrix). The EOM and EOV are integrated to be used to propagate the state forward to any observation time through a Hamming integrator. The Hamming integrator is an ordinary differential equations (ODE) integrator that uses a fourth order predictor-corrector algorithm. This type of algorithm carries along the last four values of the state vector and extrapolates the values to obtain the next value, noted as the predictor. The extrapolated value is then corrected to find a new value for the state vector. The EOM is integrated to find the state at a particular observation time, while the EOV are integrated to find the corrections to the state that need to be applied to converge on a solution.

$$\mathrm{H} = T + V = \frac{1}{2}(p_x^2 + p_y^2 + p_z^2) + \Omega_{Earth}(yp_x - xp_y) + V(x, y, z) \tag{11}$$

$$\vec{f} = \frac{\partial H}{\partial \vec{x}} = \begin{bmatrix} \dot{x} \\ \dot{y} \\ \dot{z} \\ \dot{p_x} \\ \dot{p_y} \\ \dot{p_z} \end{bmatrix} = \begin{bmatrix} \frac{\partial H}{\partial x} \\ \frac{\partial H}{\partial y} \\ \frac{\partial H}{\partial z} \\ \frac{\partial H}{\partial p_x} \\ \frac{\partial H}{\partial p_y} \\ \frac{\partial H}{\partial p_z} \end{bmatrix} = \begin{bmatrix} -\Omega_{Earth} p_y + \frac{\partial V}{\partial x} \\ -\Omega_{Earth} p_x + \frac{\partial V}{\partial y} \\ \frac{\partial V}{\partial z} \\ p_x + \Omega_{Earth} y \\ p_y - \Omega_{Earth} x \\ p_z \end{bmatrix} \tag{12}$$

$$\dot{\Phi}(t, t_0) = A(t)\Phi(t, t_0) = \frac{\partial \vec{f}}{\partial \vec{x}} \frac{\partial \vec{x}(t)}{\partial \vec{x}(t_0)} \tag{13}$$

3.2.3 Truth Data Input Types

The original SP algorithm would only allow J2000 inertial position data and MJD for time and data as input, but the modified SP algorithm can use several types of input formats for the observation and state data. The inertial data used for this research was provided through several types of truth sources: an STK generated data file, data provided from the GPIM host vehicle, or satellite position records collected by a real Earth orbiting satellite and are summarized in Table 5. For inertial data generated in STK, the input data is separated into two pieces, information specifying the parameters used to input data and an observation data for the spacecraft. The input parameter information includes where to find the observation data, a specified number of maximum iterations, the type of input source, and a specified maximum geopotential order, whereas the observation data provides the actual time, position, and velocity data of the spacecraft. As part of this research effort, the SP algorithm was modified to accept the STK format of truth data in the form of date and UTC time and an inertial position and velocity vectors.

Table 5. SP Software Input Formats

Data Name	**Data Source**	**Time and Date**	**Position**	**Additional Info**
Original	Dr. Wiesel	MJD Number	J2000 Vector	N/A
STK	STK Simulation	Date and UTC Time	J2000 Vector	J2000 Velocity Vector
SOS (GNSS)	STK Simulation & GNSS Simulator	GPZDA Sentence	GPGGA Sentence	N/A
SOS (Encoded)	STK Simulation & Algorithm	GPZDA Sentence	GPGGA Sentence	N/A
GPIM	GPIM (currently unavailable)	GPS Seconds	ECEF Vector	N/A
STPSat-3	STPSat-3 (Real World)	GPS Week & Seconds	ECEF Vector	N/A

To aid in the main focus of this thesis, the algorithm was also modified to allow GPS NMEA sentences to be used as truth data input. As previously discussed in Section 3.2.1, GPGGA and GPZDA NMEA sentences are brought in and converted to a J2000 inertial position vector and Julian day number. The GPS sentences are the expected input from SOS, whereas the host vehicle provides its observation data to SOS as an inertial vector, similar to the algorithm's original data format. The GPIM host vehicle has its own GPS receiver to collect position data which is then converted to an inertial vector on-board the spacecraft and transmitted to SOS every second as telemetry data. Through additional modification, the data format provided by the GPIM host vehicle was also added, which allowed for data to be brought in in the format of time in GPS seconds since GPS week number rollover (22 August 1999) and a J2000 inertial position vector. The SP algorithm is able to distinguish between the two types of input sources by the first line of the observation data which specifies either "SOS" or "HOST." Once the algorithm recognizes that the observation data being provided is coming from the host vehicle, the software changes its behavior to not only count the observations and read in the data, but also convert the observation data time from GPS seconds to Julian day, making sure to account for the 17 second leap second correction (as of February 2016). The algorithm must also convert the position vector from meters to kilometers for processing.

In order to determine if errors were being generated by simulating observation data, real-world data was also used for testing of the SP algorithm. The real-world data analyzed for this research includes GPS position, velocity, and time navigation data collected on orbit by STP Satellite-3 (STPSat-3) provided by the Air Force Space and Missiles System Center Spacecraft Development Branch in support of Jenson's research of the validation of the SGP4 OD algorithm. STPSat-3 flies at approximately 500 kilometers altitude and 40.5 degrees inclination. and was launched 20 November,

2013. [67] Information collected by STPSat-3 included time provided in GPS week number and week second and position vectors in the ECEF coordinate frame recorded approximately once every 30 seconds for 24 hours. Through Jenson's efforts, the position vectors were transformed from the ECEF to the ECI coordinate frames and time was converted to number of seconds since GPS week number rollover. [12] Because the position vectors needed to be in the J2000 frame for processing within the SP algorithm, the STPSat-3 GPS position vectors were rotated from ECEF to J2000. The final format modification of the real-world data used for this research encompassed modifying it to be the same format provided by the host vehicle so that it was able to be tested through the same input scheme.

Each type of input format was analyzed to test their effects on the accuracy of the SP OD algorithm. However, complications arose when the truth model propagator chosen in STK used to generate the STK input data and SOS GPS data was further analyzed and will be discussed in Section 3.3.3.

3.3 Special Perturbations Algorithm Development

The main focus of this research was to modify an existing SP Least Squares algorithm to test the achieved accuracy when using observation data from a GPS receiver in the form of NMEA sentences. Several steps had to be taken in order to correctly validate the approach and analyze the final results. Because the unmodified algorithm could only process inertial data, the first step in validation was to achieve results that were the same as those that were found using the original algorithm. Once the validation was completed, the algorithm was modified to allow inertial input data provided from STK and host vehicle. The input data provided from STK and SOS was generated from the same truth model simulated in STK as a way to reliably compare the results. This truth model was created by Jenson to validate and analyze

the results of the SGP4 algorithm used as the on-board OD algorithm for SOS. [12]

Because of the new input format, the validation of the modified code became more complicated. Errors caused by inconsistent time formatting and state correction calculations required rigorous editing and testing of the software. Specifically, checking the accuracy of the state corrections through singular value decomposition acknowledged the need to rewrite the code to use dimensionless units instead of physical units. After this modification was complete, it was discovered that although the propagation method chosen by Jenson, J4, to create the truth model orbital scenarios in STK was accurate enough to validate SGP4; it would not provide accurate enough truth data to compare to results generated by SP. Because of this, the simulated observation data used to create the STK files and SOS GPS data files had to be recreated using the HPOP propagator in STK. In order to create the SOS GPS data files, two methods were used to transform the truth model to GPS sentences. First, the inertial position vector and time in UTC was converted to both GPGGA and GPZDA sentences. As an alternative method, data was produced from the SOS Novatel OEM615 GPS receiver through the use of a Spirent GSSS8000 GNSS Simulator.

The accuracy of the position estimates produced from the modified SP Least Squares algorithm was analyzed from each of the different data sources. Specifically, the difference between the accuracy achieved by the use of inertial frame data and GPS sentence data produced by the same truth model were compared. In the end, the modified SP algorithm results are compared to those generated by SGP4 to determine if using SP on GPS navigation solutions is a viable solution to getting more accurate position estimates.

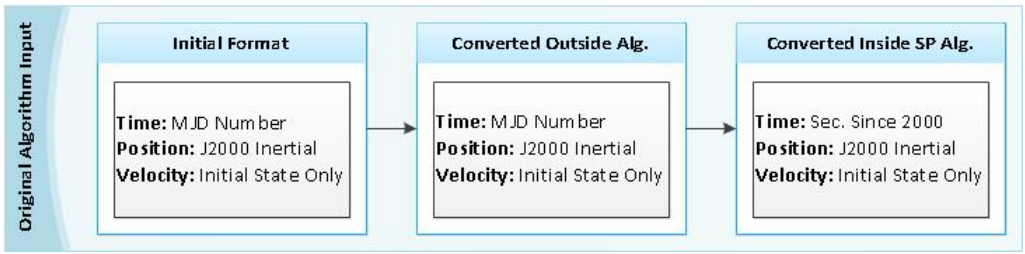

Figure 15. Original SP Algorithm Format Conversions

3.3.1 Inertial Position Input Data Validation

Part of modifying the original algorithm including adding and validating the capability to input data from the GPIM satellite and data generated from STK simulations, both of which brought in positions in the inertial frame. Figures 15 and 16 describe the processes to convert the data into the format used for calculations within the SP algorithm. Validation of algorithm's performance to process STK inertial data was tested by using orbital trajectory data previously analyzed on the SGP4 algorithm by Jenson in 2015. The STK input results generated by SP were compared to those compiled from SGP4 to provide validation. This scenario encompassed the SOS satellite at an altitude of 625 degrees and an inclination of 24.5 degrees propagated using STK's J4 propagator, already described in Table 4. Because AFIT does not have actual access to the GPIM host vehicle's GPS receiver, there was no real way to simulate this data. The validation of the processing of data provided by GPIM occurred by checking the conversion of GPS second to Julian days, since the time format is the only parameter differing from the original input format and STK simulation data shown in Figure 17. Real world data collected from STPSat-3 was provided in a form similar to the GPIM host, except it also included velocity vectors. Figure 18 explains the processes to convert the real world data for processing within the SP algorithm.

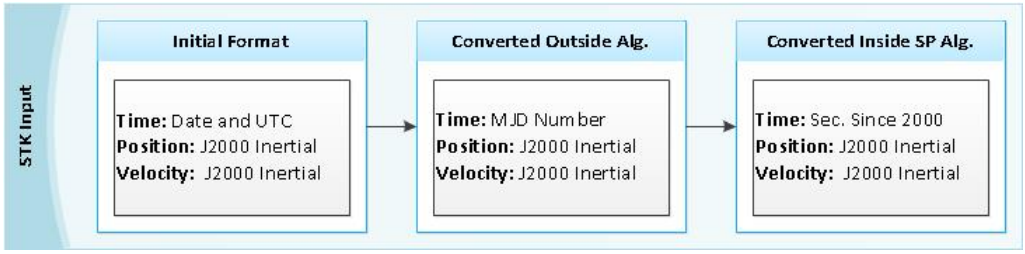

Figure 16. STK Format Conversions

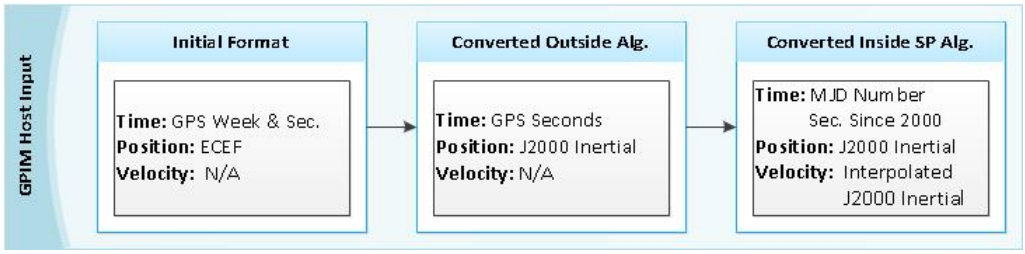

Figure 17. GPIM Host Format Conversions

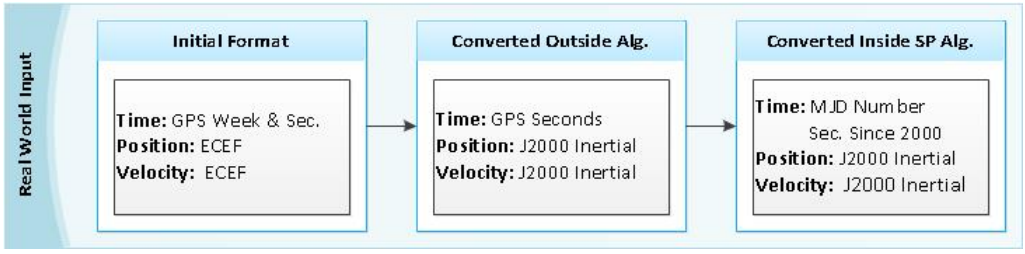

Figure 18. Real World Format Conversions

3.3.2 GPS Sentence Input Data Addition and Validation

The central efforts of this thesis were focused on modifying the SP least squares algorithm to allow for GPS sentence observation data as input. Detailed modification and validation was required within the SP least squares algorithm to work with the GPS sentence data, which was converted to the inertial frame outside of the actual SP least squares algorithm. The modifications within the algorithm to process data provided by SOS GPS sentences introduced errors that were previously not an issue when using data that was brought in already formatted to the inertial frame. This section discusses the process used to add the capability to use GPS input data and the validation process.

3.3.2.1 Algorithm Modification

Modification of the SP least squares algorithm was mainly focused on allowing GPS sentences to be used as the input state and observation data. The algorithm required modifications in order to recognize what kind of data was being processed, since only observation data was provided without input parameters, differing from data brought in from STK simulations or the original format of the algorithm. Therefore, the algorithm was modified to recognize a header in the observation data that would alert the algorithm that this observation data was being provided from SOS. When the algorithm reads this header, it recognizes that it must start the procedure of processing the SOS GPS data. Since the input parameters are not specified separately for input data coming from SOS, the number of maximum iterations and a geopotential order are directly specified within the SP algorithm as fifteen and twenty, respectively. The values chosen for these parameters were found through similar provided test.

The SP least squares algorithm also had to be modified to read in and convert

the GPS observation data to data in the J2000 inertial frame format. The conversion takes place within a separate algorithm called upon by SP, called GPS to inertial. The details of this algorithm have already been described in Section 3.2.1. Once the position vectors have been read in and converted, the inertial position vectors are assigned to an observation matrix. The time data requires further processing, however. The output of time given by the GPS to inertial conversion software is provided in the form of a Julian date. In order to process the observation data within the dynamics model and integrator, the time must be in the form of seconds since 1 January 2000, at 00:00:00 UTC. Because of this, the time output from the GPS to inertial software must be first converted from Julian days to MJD by simply subtracting 2,440,000 days. Next, the time data must be converted from MJD to the amount of seconds since 1 January 2000, at 00:00:00 UTC. The conversion process for the SOS GPS data is shown in Figure 19.

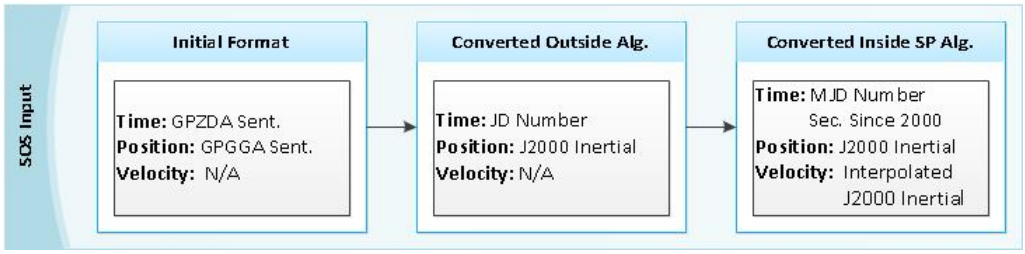

Figure 19. SOS Format Conversions

The final modification to the initial version of SP least squares algorithm required providing initial state data for the GPS data. For data provided by the original SP algorithm and STK, an initial state vector is also provided including the initial inertial position vector, inertial velocity vector, and time of epoch in MJD. The position and time data should be the same values provided in the observation data. Because the GPS NMEA sentences provided by SOS do not include velocity data, the initial velocity state must be interpolated. A three point Lagrange interpolation, described in Eq. (14), was used to fit a function to the first three inertial position data

points. Once this function was found, a velocity function was determined by taking a derivative with respect to time of the interpolated position function. Evaluating the velocity function at the epoch time provided the velocity of the initial state of the spacecraft shown in Eq. (15). After the addition of the initial state calculations, the SP software was able to begin processing the GPS data to determine an orbit prediction.

$$x(t_0) = \frac{x_0(t-t_1)(t-t_2)}{(t_0-t_1)(t_0-t_2)} + \frac{x_1(t-t_0)(t-t_2)}{(t_1-t_0)(t_1-t_2)} + \frac{x_1(t-t_0)(t-t_1)}{(t_2-t_0)(t_2-t_1)} \tag{14}$$

$$v(t_0) = \frac{(x_1-x_0)}{(t_1-t_0)} + \frac{(x_2-x_0)}{(t_2-t_0)} + \frac{(x_1-x_2)}{(t_2-t_1)} \tag{15}$$

3.3.2.2 Validation Process

Before testing of the GPS data could begin, the modified SP least squares algorithm required validation of the newly updated processes. Several steps were taken to maintain authenticity of the results provided by the SP algorithm, including testing the time formats throughout the code and the covariance matrix inversion process. Through analysis of the validation process, it was determined that the software needed to be converted from working in physical units to working in dimensionless units.

Time standards played a major role in validating the results provided by the SP algorithm. Each type of input format used different standards of time, which became very important to make sure that the correct time format was used upon input to the least squares process. Specifically for the GPS data, errors were recognized due to incorrect uses of Julian date and MJD and had to be thoroughly investigated throughout the algorithm.

Once the time formatting throughout the algorithm was validated, the matrix inversion to produce the covariance matrix was checked for correctness. This process

was completed by multiplying the inverse covariance matrix P^{-1}, found through the observation matrix T and instrument covariance matrix Q in Eq. (16), with the covariance matrix P, found from taking the inverse of the inverse covariance matrix in Eq. (17). If the matrix inversion worked correctly, this multiplication should result in the identity matrix.

$$P^{-1} = \sum_i T_i^{\mathrm{T}} Q_i^{-1} T_i \tag{16}$$

$$P = (P^{-1})^{-1} = \left(\sum_i T_i^{\mathrm{T}} Q_i^{-1} T_i \right)^{-1} \tag{17}$$

Further analysis was completed on the covariance matrix inverse by checking the rank of the matrix through singular value decomposition (SVD). Calculating the eigenvalues of P^{-1} allows for analysis of the accuracy of the state corrections. However, eigenvalue decomposition is very computationally expensive. As an alternative means for analysis, SVD is much cheaper numerically and achieves the same result. Looking at the singular values determined by SVD allows for the validation of the state corrections. If the singular values span a large number of orders of magnitude, the state corrections are not well determined. When completing these calculations with double precision numbers, the orders of magnitude between the highest and lowest singular value spanned about 11 orders of magnitude, which was very close to the precision limit of order 13 for double precision numbers. This also meant that corrections being calculated by the SP algorithm through GPS data would produce a covariance matrix with orders of magnitude of 20, since the covariance matrix is dimensionally a matrix of the eigenvalues squared. Through discussing these results with Dr. Wiesel, it was recommended to change the SP algorithm from working in physical units to working in dimensionless units based on Earth radii and standard

gravitational parameter of the Earth μ.

In order to convert the SP least squares algorithm to use dimensionless units, several steps had to be taken. The dynamics model already allowed for the use of either dimensionless or physical units, so only the calling had to be changed of which to use. Within the SP algorithm itself, the values of position, velocity, and time had to be converted from using kilometers, kilometers per second, and seconds to their respective non-dimensional counterparts. This process occurred at the moment of input data in the inertial frame for each of the different input formats. Eq. (18), (19), and (20) show how each parameter was converted from physical to dimensionless units. Debugging and validating the new software lead to the discovery of yet another error caused by time standards. A final modification required the conversion of the time step used for integration, which was calculated by finding the number of steps at a typical five second step size.

$$\text{Position Unit} = \text{Earth Radius} \tag{18}$$

$$\text{Velocity Unit} = \sqrt{\frac{\mu}{\text{Earth Radius}}} \tag{19}$$

$$\text{Time Unit} = \frac{(\text{Earth Radius})^{\frac{3}{2}}}{\sqrt{\mu}} \tag{20}$$

3.3.3 Truth Model Validation

Even after the modifications were made to the algorithm to allow for GPS input, few deviations were found between the results previously found from the SGP4 algorithm and those found using SP. Upon further analysis, it was concluded that the truth model being used to create the STK orbital scenarios and simulated GPS data

created by Jenson in 2015 was not modeled to a high enough geopotential order to match those being used within the SP algorithm. From this finding, new simulated GPS data was created from the STK scenario described in Table 4 through the use the Spirent GSSS8000 GNSS Simulator as well as a new algorithm that converts inertial data produced through STK to NMEA GPGGA and GPZDA sentences.

In support of previous research on SOS's SGP4 OD algorithm, Jenson created simulated GPS data through the use of STK and the Spirent GSSS8000 GNSS Simulator. He modeled several orbits in STK, varying in altitudes and inclinations, similar to what will be experienced by SOS in future testing described in Table 1 found in Section 1.2 . For purposes of this research, only one orbital scenario was used for testing of the SP software based on the provided results from Jenson at 625 kilometer altitude and 24.5 degree inclination with a zenith facing GPS antenna (Table 4). Because he simulated his orbital scenarios using the STK J4 propagator, the truth model is only modeled to the fourth degree of the Earth's geopotential model. Using such a low degree of geopotential for the truth data is not sufficient for use in the SP dynamics model, which models the geopotential to a specified degree of twenty. Due to this shortcoming in truth model accuracy, the simulated GPS data to be tested in the SP algorithm had to be recreated using a more accurate propagator in STK. The propagator chosen for the updated truth model was STK's HPOP propagator previously discussed in Section 3.1. HPOP also allows the user to choose which perturbations to apply to the model. For this research, only geopotential forces were applied to the system in order to match the perturbations applied in the SP dynamics model. Additional perturbations such as air drag and third body motion can be added to each of the models for future research. Once the chosen orbital scenario was updated with the new propagator in STK, a report was generated including UTC time and date and J2000 inertial position vectors. In order to create simulated GPS

data similar to that which would be created on SOS, the inertial position data and time reports were converted to GPS data in two ways, through the use of conversion software developed by Dr. Wiesel and the Spirent GSSS8000 GNSS Simulator and SOS flight model. The overall processes to convert the updated STK simulations to GPS NMEA sentences is represented in Figure 20.

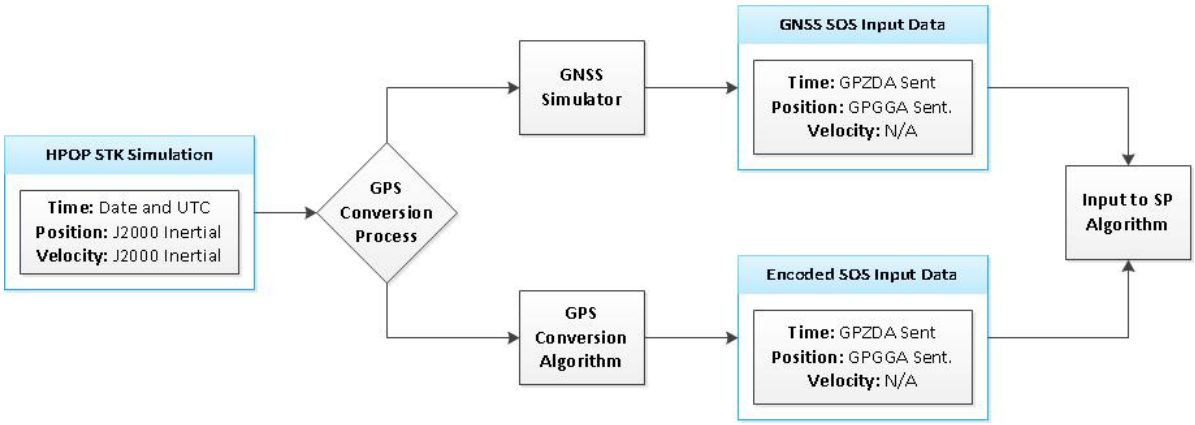

Figure 20. Processes to Convert HPOP STK Simulations to GPS NMEA Sentences

As a way to convert inertial data into simulated GPS sentences, a new algorithm was developed that in essence completes the same conversions as the GPS to inertial algorithm described in Section 3.2.1 but in the opposite order. The inertial to GPS algorithm was validated by running inertial data through it and then running the new simulated GPS data through the GPS to inertial algorithm. Validation proved successful, and the initial inertial data that was inputted into the new algorithm was also outputted through the process. Using this new algorithm allows for testing of new GPS simulated data that was now modeled from an accurate enough degree. It allows for the analysis of the formatting limitations of GPS sentence data and how it affects the accuracy of SP orbit determination. However, the effects of the GPS receiver are not able to be tested and analyzed through the use of the conversion algorithm alone.

A major part of how GPS sentence data could affect the accuracy of position

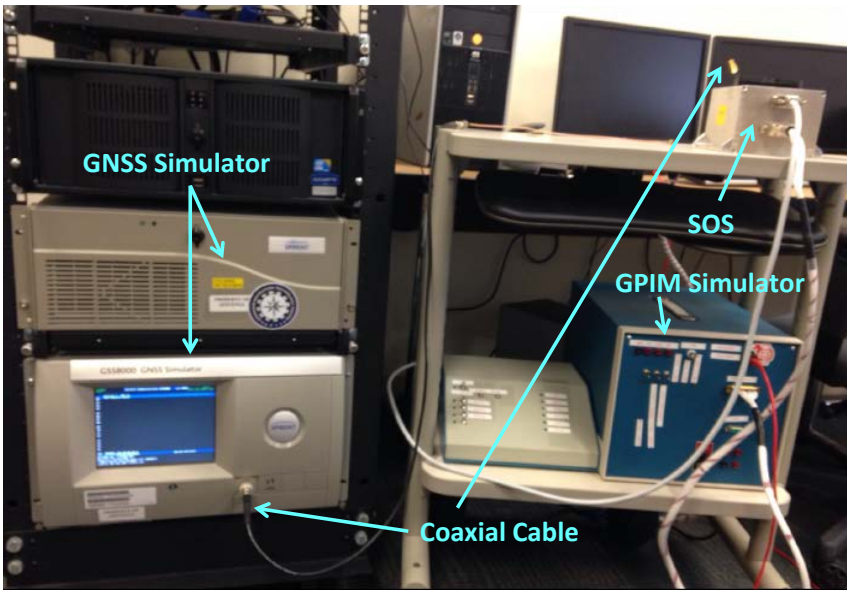

Figure 21. Setup of GNSS Simulation with SOS

estimates generated by the SP algorithm is the accuracy of the actual GPS receiver when calculating its own position estimates. In order to test this, the GNSS Simulator was connected to SOS's OEM615 GPS receiver. The GNSS simulator used for this research was loaned from AFIT's Autonomy and Navigation Technology Center. The approach used for the simulation process was derived by Jenson in 2015 for his own research [12]. The simulator was configured with Spirent's SimGEN software. The SimGEN software read in a user motion (UMT) file produced from the STK simulation, which represented the trajectories of the GPIM spacecraft and acted as the truth model for the simulator input and error characterization. The UMT file contained time, position, velocity, acceleration, and jerk expressed in ECEF coordinates along with attitude, angular velocity, angular acceleration, and angular jerk in the satellite body axes. Using the trajectory truth model, the SimGEN software simulates GPS signals to the OEM615 GPS receiver through a coaxial cable. Connecting the SOS flight model to the GPIM simulator and desktop computer allowed the GPS data to be logged into the SOS graphical user interface (GUI) through sent commands. Once

the GPS data was logged into the GUI, it was extracted from SOS's single board computer (SBC) and parsed into readable GPS sentences used for this research. The set-up of the simulated GPS data collection is shown in Figure 21.

3.4 Implementation of Experiments

Once validation of the SP least squares algorithm was complete, experiments were implemented to test the achievable accuracy of the algorithm in effect to different types of input. The algorithm's performance was tested as a result of both simulated and real-world orbital observation data. The dimensionless unit version of the SP algorithm's performance was compared to the performance of the SGP4 algorithm. Also, the accuracy obtained from J4 STK truth model was compared to the HPOP STK truth model. The accuracy of the algorithm was characterized by evaluating the position residuals produced as output from the algorithm, which were calculated by evaluating the difference between observations and estimated state data. Computation time was also evaluated to characterize the difference in performance between the dimensionless and physical unit versions of the algorithm. A summary of the tests performed is shown in Figure 22.

Computation Time Comparisons	
Test Scenario 1	**Test Scenario 2**
Physical SP Algorithm (All Data Sets)	Dimensionless SP Algorithm (All Data Sets)

Algorithm Comparisons	
Test Scenario 1	**Test Scenario 2**
J4 SGP4 GPS SOS (GNSS)	J4 SP GPS SOS (GNSS)
HPOP SGP4 GPS SOS (GNSS)	HPOP SP GPS SOS (GNSS)
SGP4 ECEF STPSat-3	SP ECEF STPSat-3

Propagator Comparisons	
Test Scenario 1	**Test Scenario 2**
J4 SP GPS SOS (GNSS)	HPOP SP GPS SOS (GNSS)
J4 SP J2000 STK	HPOP SP J2000 STK

Input Format Comparison	
Test Scenario 1	**Test Scenario 2**
HPOP SP J2000 STK	HPOP SP GPS SOS (GNSS)
HPOP SP GPS SOS (GNSS)	HPOP SP GPS SOS (Encoded)

Figure 22. Summary of Experiments

Simulated data including STK and SOS data sets originated from the orbital scenario described in Table 4 found in Section 3.1, using both J4 and HPOP propagators.

The formats for each of the simulated data sets are described in Table 5. Simulated observation data was taken from STK and converted to GPS sentence data through the process described previously in Section 3.3.3 Figure 20. Simulation time for the scenario was set to 24 December 2014 from 00:00:02 to 23:59:59 UTC in order to match the scenario used for analysis on SGP4 by Jenson. Since results of Jenson's analysis on SGP4 recommended that a sampling rate of once per minute for a duration of 24 hours was necessary for sufficient algorithm performance on SGP4, the same sampling rate and duration was used for analysis of SP. By specifying this sampling rate and duration in the SOS GUI when creating the GPS data through the simulator, the testing duration resulted in the output of 24 December 2014 00:06:54 to 23:57:29 UTC. Subsequent STK inertial observation data being evaluated was set to a testing duration of 24 December 2014 00:06:54 to 23:57:54 UTC at a one minute sampling rate as a way to create a valid comparison to the GNSS data. Using the STK inertial observation data, another set of GPS sentence testing data was created using the conversion algorithm described in Section 3.3.3. As previously mentioned, real-world observation data from STPSat-3 was provided from Jenson's 2015 research efforts [12], except modified for SP algorithm testing to be sampled every 30 seconds for 24 hours as it was originally presented from STPSat-3. Jenson's analysis on SGP4 used a sampling rate and duration of the observations of once per minute for eight hours. Jenson attempted to always place the last data point of his sampled real-world data sets to the epoch time of the official JSpOC TLE used as a truth reference. However, this point landed at 7 January 2015 at 00:20:12.622 UTC and fell near the middle of the real-world data set, explaining why only eight hours of data was evaluated instead of twenty four. Because analysis of the SP algorithm included examination of position residuals and not TLEs, the full data set from STPSat-3 was able to be used for SP algorithm analysis. A summary of the testing times for each

experiment is shown in Figure 23.

Data Source	Testing Scenario	Test Start Time		Test End Time	
		Date	Time	Date	Time
STK J4	SGP4 GPS SOS (GNSS)	24-Dec-2014	0:01:50	25-Dec-2014	0:46:50
	SP GPS SOS (GNSS)	24-Dec-2014	0:01:50	25-Dec-2014	0:46:50
	SP J2000 STK	24-Dec-2014	0:06:54	24-Dec-2014	23:57:54
STK HPOP	SGP4 GPS SOS (GNSS)	24-Dec-2014	0:06:54	24-Dec-2014	23:57:29
	SP GPS SOS (GNSS)	24-Dec-2014	0:06:54	24-Dec-2014	23:57:29
	SP GPS SOS (Encoded)	24-Dec-2014	0:06:54	24-Dec-2014	23:57:54
	SP J2000 STK	24-Dec-2014	0:06:54	24-Dec-2014	23:57:54
STPSat-3	SGP4 Real World	6-Jan-2015	16:19:12	7-Jan-2015	0:20:09
	SP Real World	6-Jan-2015	15:59:21	7-Jan-2015	15:59:02

Figure 23. Summary of Testing Durations for Each Experimental Data Set

The SP OD algorithm provided results for analysis in the form of position residuals in the radial, along track, and cross track orbital directions. Both the plots of the position residuals and the overall root mean square (RMS) residual in each testing scenario were used as methods to analyze the results of the algorithm. Each testing scenario was assessed in both the physical units and dimensionless units versions of the software. Specifically, the total computation time to solution convergence was tracked in each of the software versions. Figure 12 in Section 3.1 summarizes the experiments completed for this research and the results produced. The results of each of these tests are discussed in Chapter IV.

4. Results and Analysis

This chapter presents the experimental results and analyses as described in the previous chapter. The accuracy of the position estimates determined in each test case are analyzed through the calculation of position residuals, which describe the difference between the observed position values and the estimated state values in the radial, cross track, and along track orbital directions. Each simulated test case – data compiled from STK, the GNSS simulator, or STK converted GPS data – is composed of data sampled once per minute for a duration of 24 hours. The data collected from STP-Sat3 was down sampled during Jensons research and is composed of samples taken once per minute for eight hours and will be referred to as real-world data. Using the effects of using physical units versus dimensionless units for the determination of position estimates and residuals are discussed. Building upon the outcome of that analysis, position residual results based on the calculations performed in dimensionless units are studied. These position residuals are calculated from data provided by STK, GNSS simulations, and conversion software developed from both J4 and HPOP truth models. Using data provided by STP-Sat3, the residual products of SP and SGP4 based on real-world data are examined.

4.1 Effects of Dimensionless versus Physical Units

In order to complete analysis on the SP least squares algorithm, several test cases were analyzed using two versions of the algorithm that calculate the state estimates in either physical or dimensionless units. The conversion from physical to dimensionless units was initiated during the validation phase of the modified SP least squares algorithm and specifically examining the values of the inverse covariance matrix. During this process, it was determined that the state estimates being produced were not

accurately known in all directions of the state space when using physical units. This conclusion was made by analyzing the singular values produced through SVD of the inverse covariance matrix since the range between the largest and smallest number was on the order of 11 in magnitude for all test cases. After this realization, the SP algorithm was converted to run in dimensionless units. This conversion resulted in SVD singular values ranging by an order of five in magnitude for all test cases, meaning that the state estimates in all directions of the state space were more accurately known.

Table 6. Position Residuals Results

	Physical: RMS Residual (km)	**Dimensionless: RMS Residual (km)**
J4 SP J2000 STK	7.0598099	7.0597924
HPOP SP J2000 STK	0.2418617	0.2418648
J4 SGP4 GPS SOS (GNSS)	6.9554561	N/A
J4 SP GPS SOS (GNSS)	6.9805246	6.9805150
HPOP SP GPS SOS (GNSS)	0.3380191	0.3380214
HPOP SP GPS SOS (Encoded)	0.2418620	0.2418650
SP ECEF STPSat-3	0.6507791	0.6474034
SGP4 ECEF STPSat-3	0.3351203	N/A

By completing the conversion from physical to dimensionless units, the SP algorithm was able to calculate state estimates that were 55 percent more confidently

determined than those found through the use of physical units. This confidence value was determined by examining the decrease in SVD range from using physical to dimensionless units for each of the test cases. The residuals from each of the test cases did not show much change from the conversion of code, but by analyzing the SVD singular values, it can be concluded that one can be much more confident in the residual values represented by using the dimensionless units SP algorithm. A summary of the residual values for each of the test cases calculated by both physical and dimensionless units is presented in Table 6. A more detailed discussion on the comparison of the position residuals for different test cases is presented in the following sections.

Not only did the conversion of the algorithm provide better state estimates, but it also significantly reduced the processing time of the algorithm. Using system timestamp outputs in each of the algorithm test cases provided the means to analyze the total processing time for each of the test scenarios. For each scenario, the algorithm processing time was recorded in three tests and averaged to compute the percent increase in processing speed resulting from switching from physical units to dimensionless units. Table 7 summarizes the results for each testing scenario. By completing the conversion of the algorithm, processing speeds increased by an average of 30 percent out of three runs. This increase in speed is significant when considering the use of this algorithm onboard a spacecraft.

4.2 J4 Propagation Orbit Determination

In order to provide a valid comparison between the results generated from this thesis using the modified SP algorithm and those found previously by Jenson using the SGP4 algorithm, attempts were made to test the same simulated data that was used by Jenson [12]. According to Table 5, simulated data, including data STK J2000 inertial data and both types of SOS GPS data, was created in STK using the

Table 7. Physical versus Dimensionless Units Processing Runtimes Analysis

	Physical Units Average Runtime (sec)	Dimensionless Units Average Runtime (sec)	Increase in Processing Speed (%)
J4 SP J2000 STK	175	113	35%
HPOP SP J2000 STK	140	78	45%
J4 SP GPS SOS (GNSS)	230	180	22%
HPOP SP GPS SOS (GNSS)	168	137	18%
HPOP SP GPS SOS (Encoded)	168	134	21%
SP ECEF STPSat-3	207	130	37%
Overall Average	**179**	**129**	**30%**

J4 propagator. This section discusses the analysis of results generated from the SP algorithm compared to those found previously using SGP4 when the simulated input originated from the J4 propagator.

The results generated from the SP algorithm using J4 simulated data as input only varied by about 80 to 100 meters between input formatted in the inertial frame and those formatted in GPS sentences. Specifically, there were little noted effects caused by the processing of a navigation solution within the GPS receiver which would have been evident in the GNSS simulator residuals. The RMS residuals generated from both STK data and data fed into the GNSS simulator showed very little bias, both lying around 7 kilometers. Also, both data sets showed a radial position residual bias around 7 kilometers. Figures 24 and 25 display plots of the position residuals for the STK data and GNSS simulated data, respectively. It can be noted that these plots look almost identical, which means that this data really does not provide much insight into the effects of using the GPS navigation solution to formulate state estimates through the SP algorithm.

Comparing the results generated from the SP algorithm to those found from Jen-

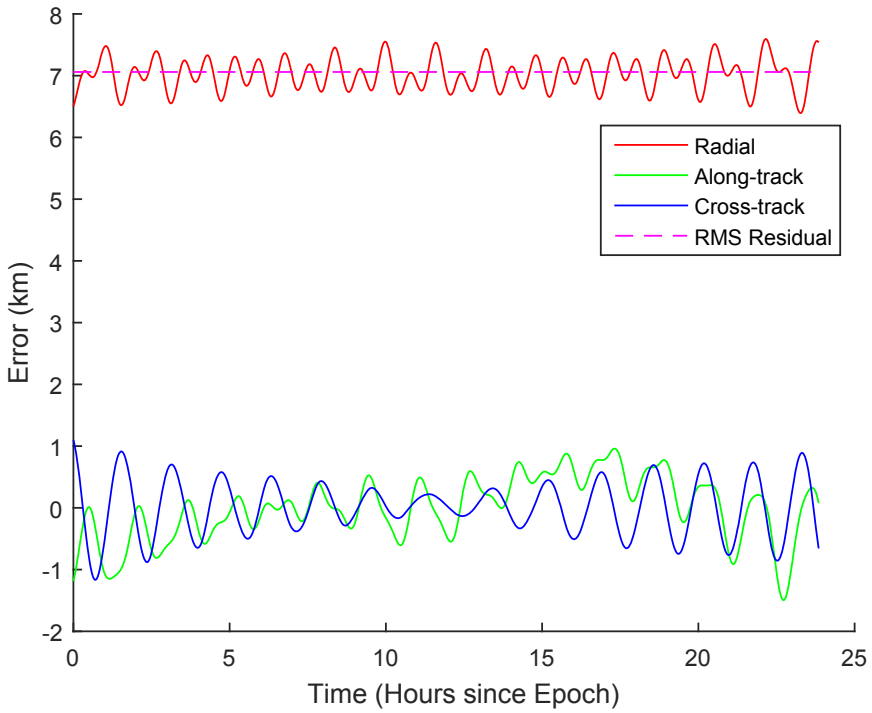

Figure 24. J4 STK Inertial Data SP Position Residuals

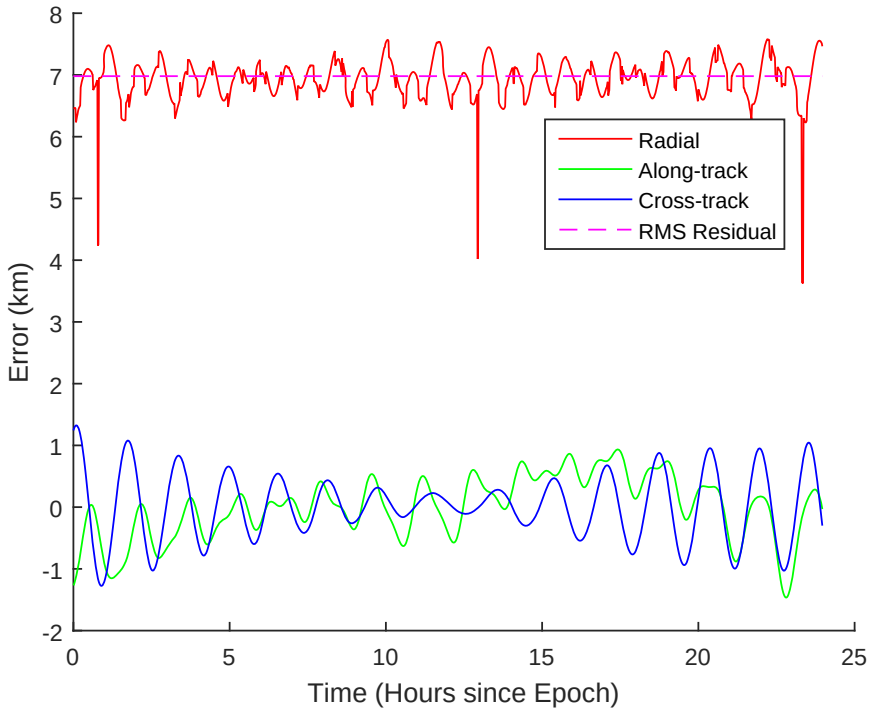

Figure 25. J4 GNSS Simulator GPS Data SP Position Residuals

son using SGP4 also showed almost no deviations in the accuracy of the estimates. Examining the results found by Jenson in Figure 26 also displays very little variation compared to those shown above. [12] It should be noted that this plot was newly generated using the previous results in order to match the formats used throughout this thesis. Table 8 summarizes the RMS residuals determined in each of the testing scenarios. Using J4 as the truth model for data fed into the SP algorithm actually decreased the accuracy from the results determined through SGP4 by up to 1.5 percent. Because of this, conclusions were drawn that J4 would not provide any additional value to the analysis of the SP algorithm. Instead, HPOP simulations were created to conduct further testing.

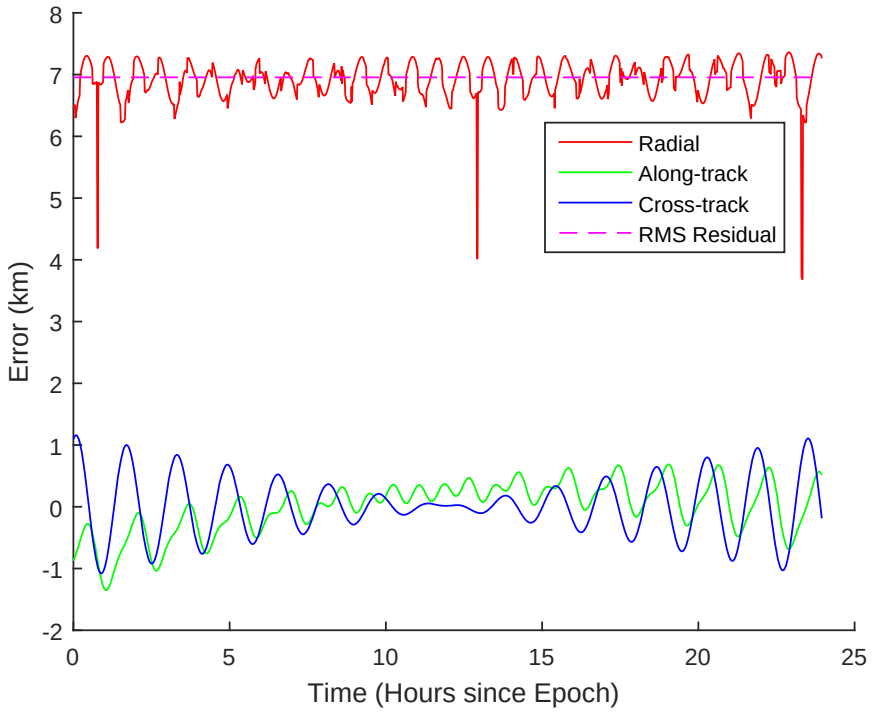

Figure 26. GNSS Simulator GPS Data SGP4 Position Residuals [12]

Table 8. J4: Percent Accuracy Increase from SGP4 Results Analysis

	RMS Residual (km)	Increase in Accuracy from SGP4 (%)
SGP4 GPS SOS (GNSS)	6.9554561	N/A
SP J2000 STK	7.0598099	-1.50%
SP GPS SOS (GNSS)	6.9805246	-0.36%

4.3 HPOP Propagation Orbit Determination

Because propagating the truth model using classical orbital elements in STK with HPOP allowed for user input to be provided on perturbation parameters, analysis showed that state estimates resulted in much more accurate results. The perturbations applied to the truth model in STK included an Earth geopotential model to order 20 and excluded air drag, solar radiation pressure, or forces due to the third body motion of the Sun or Moon rather than simply the fourth order geopotential model provided with J4. This decision was made in order to closely match the perturbations applied within the dynamics model of SP algorithm. The effects of changing the truth model propagator to HPOP on the accuracy of the SP algorithm are discussed in the following section, specifically comparing the updated HPOP results from the SP algorithm to results found from data originating from a J4 truth model and results found using the SGP4 OD algorithm.

Generating state estimates in the SP OD algorithm using simulated date, time, and position data originating from HPOP truth models provided much more interesting results than those found previously. The SP algorithm was tested using input from inertial STK data, converted GPS STK data, and GPS data provided by the GNSS simulator and SOS, all originating from an HPOP STK truth model. By using these three different types of simulated data sets, the effects of input reference frame and the use of GPS receiver navigation solution input were able to be investigated

and analyzed.

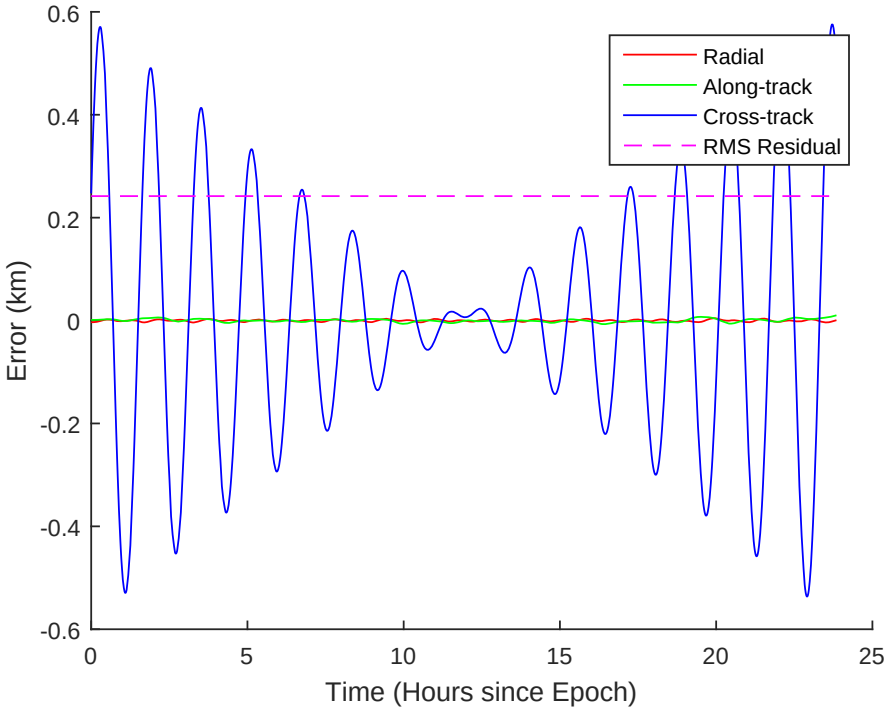

Figure 27. HPOP STK Inertial Data SP Position Residuals

Position residuals resulting from the use of J2000 inertial frame data and data converted from the J2000 inertial frame to GPS NMEA sentences showed very similar errors, shown in Figures 27 and 28. It can be noted that the position residuals overall display much smaller errors than those presented by data provided by the J4 simulation. The average RMS residual in each of these scenarios results in a state estimate error of about 300 meters, mostly biased towards the cross track orbital direction. The "'bow-tie"' effect shown by the cross track orbital direction is most likely due to an orbital plane error that may have occurred during the conversion to sidereal time, but needs to be investigated further as future work. A summary of the RMS position residuals calculated in each of the HPOP testing scenarios is shown in Table 9. The conversion from the inertial frame to GPS NMEA sentences only resulted in a change of RMS residual error of about 0.02 centimeters. By analyzing

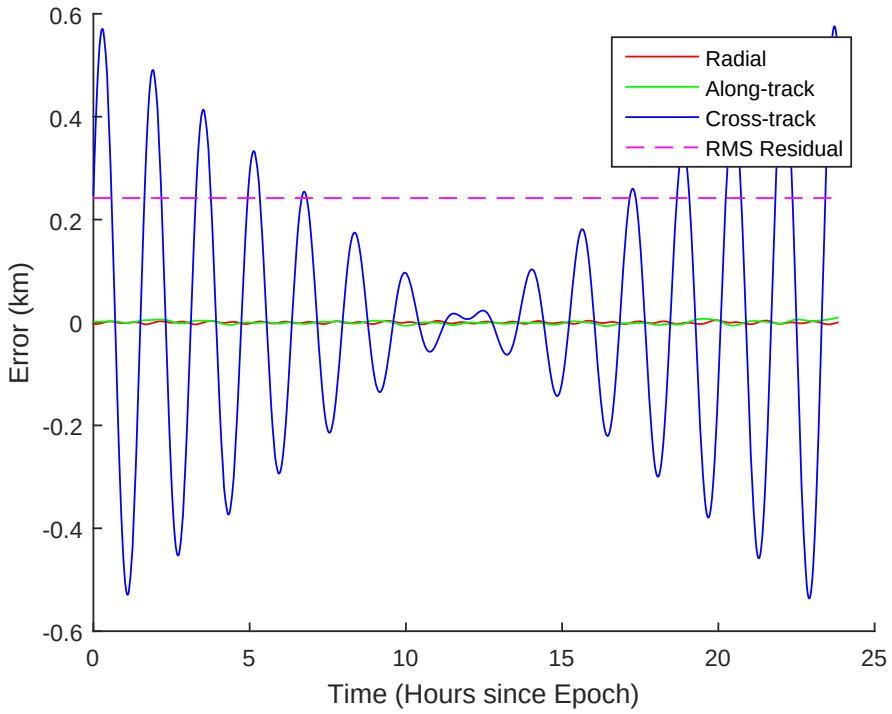

Figure 28. HPOP Converted GPS Data SP Position Residuals

this result, it can be shown that the format of GPS NMEA sentences themselves do not hinder that accuracy of the SP algorithm as it is currently in use.

Conducting further testing of the SP algorithm using the SOS GPS receiver navigation solutions through the GNSS simulator provided more valuable insight into the effects of input type on the algorithm. Errors in the state estimates increased by almost 100 meters as a result of the GPS navigation solutions, as shown in Figure 29. This can be a consequence of errors in the GPS navigation solution itself caused by issues such as the GPS receiver not being able to lock onto the GPS signal which would cause a loss of data for that amount of time. An example of this type of occurrence is represented in Figure 29 where the plot of the radial residual error changes drastically to almost 3 kilometers. While the errors in the cross-track and along-track orbital directions remain relatively the same, the errors in the radial direction grew due to the GPS navigation solutions.

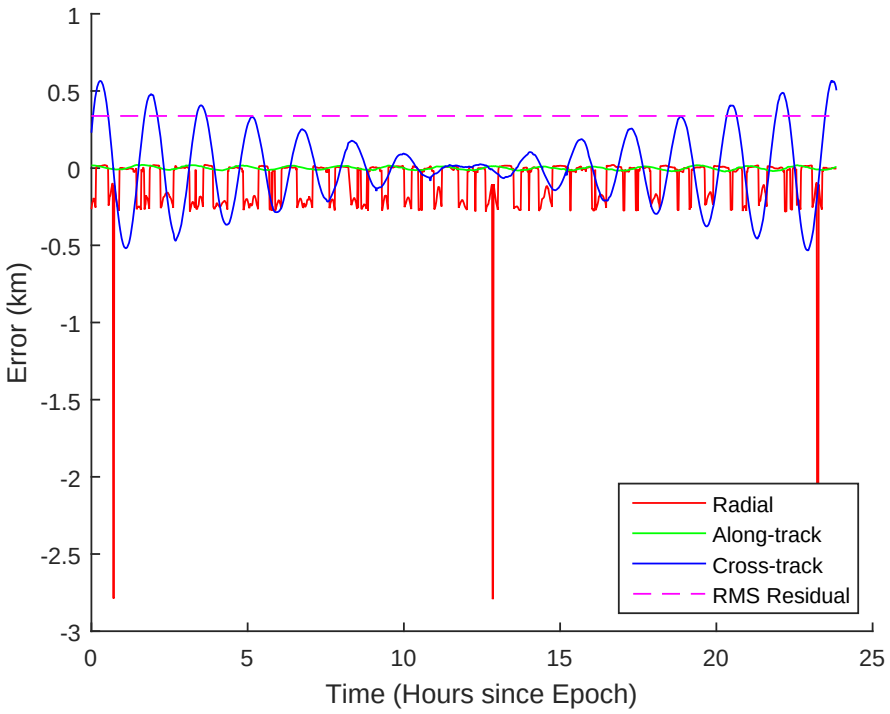

Figure 29. HPOP GNSS Simulator GPS Data SP Position Residuals

Further investigation of the position residuals generated from using simulated data derived from an HPOP truth model showed a significant increase in accuracy from both J4 and SGP4 results, summarized in Table 9. Overall, errors in the state estimates went from around seven kilometers to about 300 meters when comparing the SP results to results found using J4 or SGP4. Changing the truth model propagation greatly increased the accuracy of the estimates, by almost 96 percent. Using a more accurate STK HPOP truth model also increased the results of the SGP4 OD algorithm drastically, which was previously determined by Jenson. [12] Although this was already determined for a different set of data, the HPOP sample data for this thesis was processed through SGP4 in order to get an accurate comparison of the data. Using a new truth model in SGP4 increased its accuracy to about 93 percent, resulting mostly from the elimination of the radial position error bias. Determining state estimates using SP over SGP4 increases the accuracy of the estimate by about

42 percent on average. By adding errors that may be introduced by the GPS receiver, the increase in accuracy by using SP increased by only 28 percent. It should be noted, however, that the dynamics within the SGP4 dynamics model included air drag, the effects of which are discussed in Section 2.2.1.2, while SP did not. Because SOS will operate in LEO, adding perturbations due to air drag to the SP algorithm would greatly increase the accuracy of the state estimates which is suggested as future work.

Table 9. HPOP: Percent Accuracy Increase from SGP4 and J4 Results

	RMS Residual (m)	**SGP4**	**J4**
SGP4 GPS SOS (GNSS)	470.9015	N/A	N/A
SP J2000 STK	241.8617	48.64%	86.33%
SP GPS SOS (GNSS)	338.0191	28.22%	86.37%
SP GPS SOS (Encoded)	241.8620	48.64%	N/A

Although it has already been determined by several other sources, described in Chapter 2, that SP is more accurate than SGP4, the question remained whether or not its superiority would remain in cases where errors caused by GPS navigation solution estimates were introduced. The increasing accuracies demonstrated by these simulations prove that the SP algorithm increases the accuracy of estimates compared to those found by SGP4 and could be beneficial to the SOS mission. By only geopotential forces were applied in the SP dynamics model, the accuracy may have been hindered, however. If the SP algorithm be modified to also include effects of air drag, solar radiation pressure, and forces due to the third body motion of the Sun and Moon, the increase in state estimate accuracy may grow significantly, especially at low altitudes which may experience a significant amount of perturbations due to air drag. Once modified, the SP algorithm could be used either as a means of further processing of GPS data received on the ground or could even be exchanged as the flight software if found to be efficient enough. By converting SP algorithm into

dimensionless units, the algorithm became much more efficient when processing estimates. This conversion may provide the efficiency necessary for use on-board the SOS spacecraft. However, the testing of actual GPS data taken onboard a satellite needs to take place to truly test the performance of the SP algorithm without the effects of a simulation affected the data. The results from this procedure are described in the next section.

4.4 STPSat-3 Data Orbit Determination

The results produced by the SP algorithm using real world GPS data did not exhibit expected levels of accuracy, especially when compared to those found when using SGP4. Table 10 summarizes the RMS position residuals found when testing GPS position, velocity, and time data from STPSat-3. It should be noted that the data tested by SP needed to include positions in the J2000 frame. Because of this, the data set evaluated in the SP algorithm included 24 hours of newly converted observations, while the data set used in SGP4 by Jenson only included 8 hours of data and was evaluated in the ECI frame. None the less, the position residuals calculated by the SP algorithm demonstrated errors around 650 meters, decreasing the estimate accuracy by 93 percent from SGP4. Examining Figures 30 and 31, which show the plots of the position residuals evaluated by SP and SGP4, respectively, show much better looking results than those found by testing the simulations. There are no notable trends in any of the orbital directions for the SP algorithm position residuals. However, the SGP4 position residuals show a growth in error as time increases. This growth is most likely due to the fact that perturbations due to air drag are included in the SGP4 dynamics model, but not in the SP dynamics model.

The results produced by this particular SP approach are troubling, but do bring out some characteristics of the SP algorithm that were not able to be directly shown

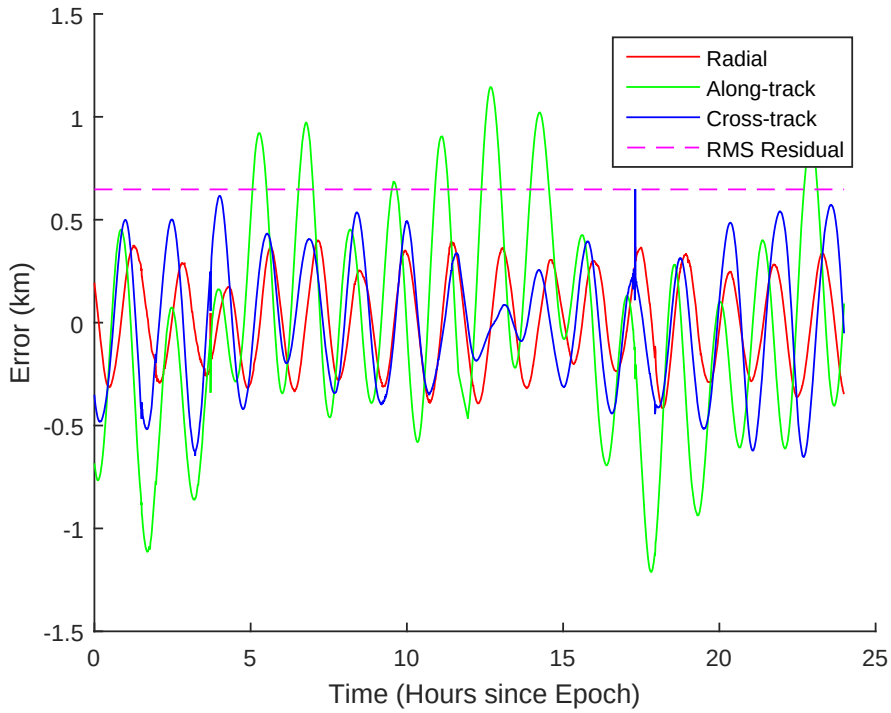

Figure 30. STP-Sat3 Data SP Position Residuals

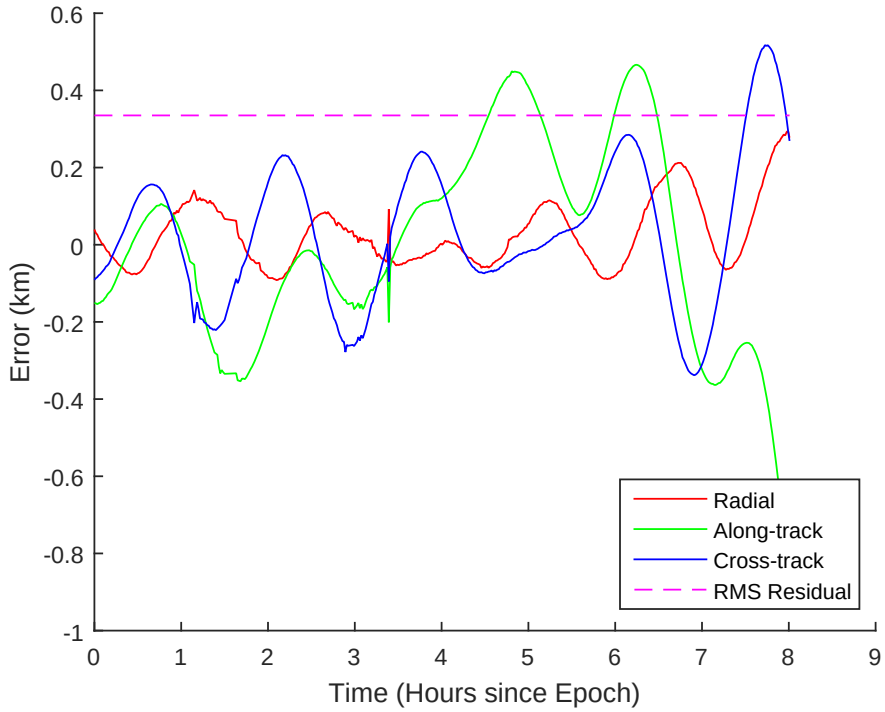

Figure 31. STP-Sat3 Data SGP4 Position Residuals

Table 10. STPSat-3: Percent Accuracy Increase from SGP4

	RMS Residual (m)	SGP4 (%)
SGP4 ECEF STPSat-3	335.1203	N/A
SP ECEF STPSat-3	647.4034	-93.19

using simulations. Inadequacies within the SP algorithm may most likely be rooted in the dynamics model and applied perturbations. Atmospheric drag is one of the largest perturbing forces on a satellite in LEO and would greatly affect the orbit of the STPSat-3 flying at an altitude of 500 kilometers. By propagating the STPSat-3 orbit found in the collected GPS data in STK using HPOP, the difference in satellite position due to air drag perturbations was demonstrated and is shown in Figure 32. The calculated distance between the satellites with and without drag in their propagation calculations is approximately 105 kilometers. An error in position of this magnitude would most definitely cause large residuals when estimating the state. Therefore, comparing the results of the two algorithms is not a completely accurate representation of the achievable performance difference between the algorithms.

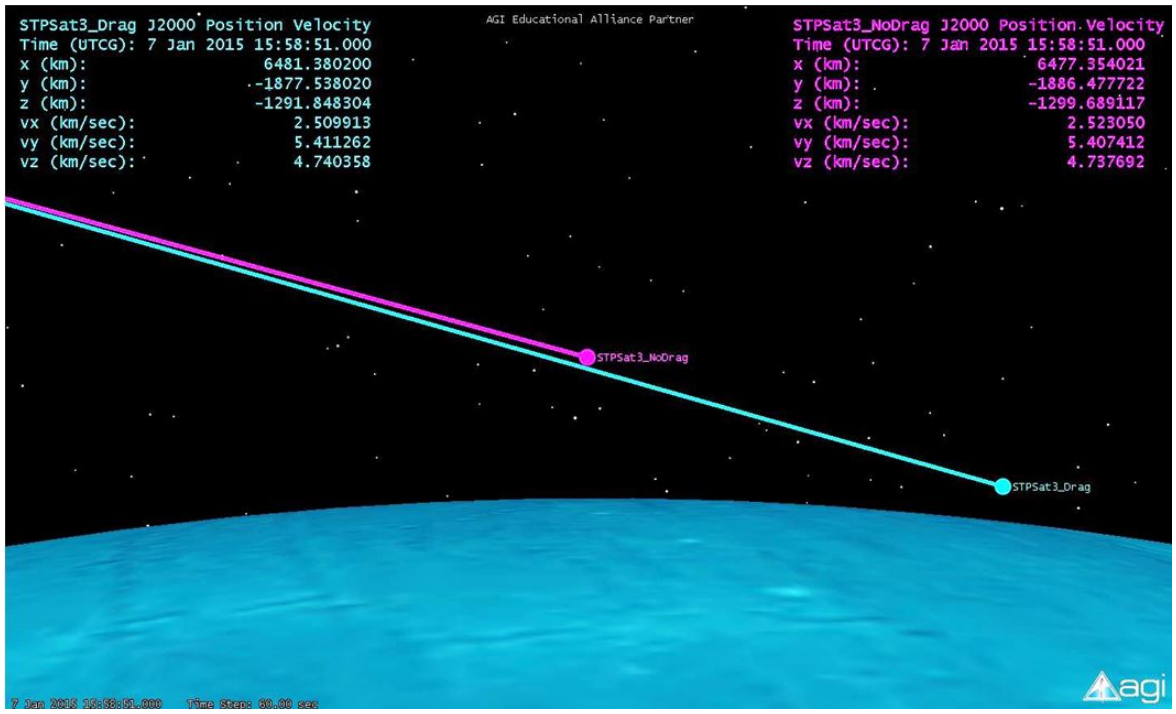

Figure 32. STPSat-3 Orbits With and Without Air Drag

5. Conclusions

This chapter provides a summary of the research and analysis performed for this thesis. It continues by describing conclusions and implications drawn from the results and analysis discussed in Chapter 4. The significance of the research performed in this thesis is discussed as well as recommendations for future work.

5.1 Research Summary and Conclusions

Currently scheduled to launch in the first quarter of 2017, the SOS experimental payload was designed as a SSA technology demonstration whose main concept of operations is to collect its own position data using a GPS receiver, perform on-board orbit determination, and transmit an estimated orbital state to the ground through the Iridium network. The focus of this research was to investigate the use of a SP orbit determination algorithm as an alternative method of orbit determination for the SOS mission by specifically studying the effects of using input GPS data on the accuracy of the estimated state. Completing this research involved modifying an existing SP algorithm to allow for GPS observation and state input data and analyzing how this change affected the accuracy of the estimated state.

To complete this research, the basic understanding of current satellite tracking methods, orbital determination, time standards, and relevant efforts were necessary and are presented in Chapter 2 of this thesis. The SP algorithm modified and analyzed in this research involves using numerical integration, non-linear iterative least squares, and a dynamics model, which models the perturbing forces applied to a spacecraft, to estimate the position and velocity of a spacecraft at an instance in time in order to accurately track the spacecraft.

By testing several orbital trajectory scenarios, both simulated and collected from

a real satellite (STPSat-3), the accuracy of the algorithm was able to be analyzed by examining the position residuals calculated by the algorithm. Simulated orbital trajectories used for observation data were conducted in STK and converted into NMEA GPS sentences through the use of both conversion algorithms and a GNSS simulator connected to the SOS GPS receiver in order to calculate and store GPS navigation solutions. Each simulation method was created using the J4 and HPOP STK propagators as truth models. By examining the difference in accuracy of GPS data originating from either the GNSS simulator, which accounted for GPS receiver errors, or converted STK J2000 data, which did not account for GPS receiver errors, the effects of the GPS navigation solution were able to be analyzed. Real GPS data collected from STPSat-3 was also analyzed. In each of the orbital scenario tests, the results found from the modfied SP OD algorithm were compared and analyzed against those found previously by Jenson [12] in 2015 using the SGP4 OD algorithm.

By modifying the SP algorithm to perform in dimensionless units instead of physical units, the algorithm performed approximately 30 percent faster. Examining the singular values generated by SVD of the inverse covariance matrix showed that using dimensionless units in the SP algorithm decreased the range of singular values from 11 orders of magnitude to 5 orders of magnitude, meaning the estimates were more confidently known in all directions of state space. The dimensionless units version of the SP algorithm provided state estimates with a 55 percent higher confidence in the provided estimations.

The results provided by the SP algorithm were highly dependent on the truth model used to create the simulated orbital scenarios. The SP algorithm was able to provide more accurate state estimations than those found by SGP4 by about 41 percent, but only when the tested simulated orbital scenarios were created using the HPOP truth model since the J4 propagator did not model perturbations to a high

enough degree. By switching the truth model propagator from J4 to HPOP, the RMS position residuals increased by almost 96 percent when using the SP OD algorithm, providing RMS position residuals near 275 meters instead of the 7 kilometer RMS residual found with J4. Changing the truth model to HPOP also eliminated the radial direction error bias. The effects of using the navigation solutions collected from the SOS GPS receiver were modeled in a decrease in the RMS position residuals to 338 meters, resulting in a 28 percent decrease in accuracy. This implies that errors were introduced into the observation data by using the GPS navigation solutions instead of raw pseudorange GPS data. Through analysis of GPS NMEA sentences generated by a conversion algorithm instead of a GPS receiver, it was determined that the errors produced by the GPS navigation solutions were most likely not due to formatting restrictions of the GPS NMEA sentences.

Using real world GPS data collected from STPSat-3 allowed for the analysis of the effects of using navigation solution data without introducing errors generated from the simulated truth model. However, testing the SP algorithm with real world GPS data resulted in a decreased accuracy when compared to SGP4 of about 93 percent, increasing in error from 335 meters to 647 meters. These poor results were most likely caused by the absence of air drag perturbations within the SP model, while SGP4 did include these effects. It is believed that modifying the SP algorithm to include air drag would most likely result in much more accurately known orbital estimates for STPSat-3. More information of the methodology used and results and analysis performed are described in Chapters 3 and 4, respectively.

5.2 Research Significance

This research has provided validation of a modified SP iterative least squares algorithm which allows GPS navigation solution NMEA sentences to be used as its

observation and state data input. It is widely known that using SP algorithms to estimate orbital states is more accurate than SGP4 algorithm. However, the effects of using GPS navigation solution observation data instead of raw GPS pseudoranges in a SP algorithm had not been extensively researched, as discussed in Section 2.4.2. Through the research conducted for this thesis, it has been shown that using navigation solutions provided by a GPS receiver on-board a spacecraft can affect the achievable accuracy of the SP algorithm. However, it was shown that although the accuracy was hindered, the SP algorithm still provided an improvement to the results compared to those found using an SGP4 algorithm when using simulated data. It was also determined that using dimensionless units for calculations within the SP algorithm increased its efficiency and performance. The results and analysis provided within this thesis can significantly contribute to the SOS mission and SSA. Once the SP algorithm has been updated to include other perturbations, especially air drag for satellites flying in LEO, it can be used as either further ground processing software or an alternative on-board OD algorithm for the SOS mission to provide more accurate state estimates than those provided by the current SGP4 flight software. By increasing the accuracy of the orbital estimates of a spacecraft, the SP algorithm studied in this thesis can be used can be used to track RSOs and aid in future conjunction analysis while utilizing the emerging technology of space-based GPS receivers flown on LEO satellites. Implementing this technology on future missions can increase the safety of RSOs and improve SSA, especially by implementing the recommendations for future research discussed in the next section.

5.3 Recommendations for Future Research

Recommendations for future work related to the research conducted in this thesis involve improving the accuracy and efficiency of the SP OD algorithm. There are

several improvements that can be completed on the algorithm which could increase the speed and decrease manual input while using the algorithm. Also, further testing could be performed with an updated SP algorithm on hardware to test how the algorithm could perform on-board a spacecraft.

In order to improve the accuracy of the SP algorithm, perturbations due to air drag and forces and third body motion of the Sun and Moon should be implemented in the algorithm. The SP algorithm itself must be changed to incorporate these perturbations. Specifically, modifications would have to be made to calculate the ballistic coefficient B^* for the GPS observation data, which would need to include the coefficient of drag, area, and mass of the spacecraft. The ballistic coefficient would have to be another element of the state that would need to be estimated by the algorithm. Adding perturbations due to air drag could significantly increase the accuracy of the algorithm, especially for satellites flying in LEO. Although third body motion is not a significant force in LEO, adding these perturbations could also increase the accuracy of the algorithm. Modifications to the SP algorithm may be necessary to address errors in the cross track orbit plane represented in the simulated data results in Ch. 4. These errors may be due to an improper conversion of time in the algorithm, as the error in the orbit plane seems to rotate one full rotation in about 98.5 years or about a century. However, more investigation into this error is required. Other modifications to the algorithm may also be necessary to deal with errors presented due to the use of GPS data, specifically accounting for the way the GPS navigation solutions are calculated within the GPS receiver. Accounting for all of these possible errors within the SP algorithm may lead to computation times that would be too long to be used on-board the spacecraft, but ground-based processing of the GPS navigation solution would still be a viable and valuable option.

Improvements to the algorithm could also be made to increase the efficiency if

previous estimates were available. By initializing the algorithm from previous estimates using a Kalman filter, the initial state of the spacecraft would not need to be estimated and could increase computation time for convergence. Also, the data tested in this thesis was manipulated to remove any data points which provided insufficient information, such as instances where the GPS NMEA sentence was empty due to loss of GPS signal. Adding code to the algorithm to get rid of this data autonomously instead of manually will make the algorithm less manually intensive and will make it ready to use on-board spacecraft. Testing the algorithm's ability to reach convergence given data over a smaller duration of time and at longer sampling rates may also lead to an increase in efficiency of the algorithm while providing savings to power consumption to a satellite if a GPS receiver was used less frequently.

To provide further analysis of the SP algorithm, testing could be performed using orbital scenarios outside of those found in the SOS mission to characterize performance at different altitudes and inclinations for a more general application. Finally, an early objective of this research included testing the SP algorithm on-board the SOS flight model SBC. The algorithms performance could be characterized in terms of computational speeds compared to those of the SGP4 algorithm. Testing could also be completed on a new command and data handling system developed at AFIT, a Beagle Board BeagleBone Black (BBB) modified to become industrial rated. Testing the SP algorithm on the spacecraft hardware will provide the analysis needed to determine if the SP algorithm can be used on-board the spacecraft or if computation time will hinder the SP algorithm to only be used as ground-based processing.

Appendix A. Acronym List

AFIT	Air Force Institute of Technology
AFRL	Air Force Research Laboratory
AFRL/RV	Air Force Research Laboratory Space Vehicle Directorate
AFSCN	Air Force Satellite Control Network
AGI	Analytical Graphics Incorporated
APL	Applied Physics Laboratory
ASAT	Antisatellite
C/A	Course Acquisition
CCAS	Cape Canaveral Air Station
CDMA	Code Division Multiple Access
CHAMP	CHAllenging Minisatellite Payload
CNES	Centre National d-Etudes Spatiales
DOD	Department of Defense
ECEF	Earth-centered Earth Fixed
ECI	Earth-centered Inertial
EELV	Evolved Expendable Launch Vehicle
EOM	Equations of Motion
EOV	Equations of Variation
ET	Ephemeris Time
FEA	Finite Element Analysis
GCT	Greenwich Civil Time
GEODSS	Ground-Based Electro-Optical Deep Space Surveillance
GEONS	GPS-Enhanced Onboard Navigation System
GIPSY OASIS II	GNSS-Inferred Positioning System and Orbit Analysis Simulation Software
GMT	Greenwich Mean Time
GNS	GPS Navigation System
GNSS	Global Navigation Satellite System
GPIM	Green Propellant Infusion Mission
GPS	Global Positioning System
GRACE	Gravity Recovery and Climate Experiment
GSFC	Goddard Space Flight Center
GUI	Graphical User Interface
HPOP	High-Precision Orbit Propagator
IAU	International Astronomical Union

ISR	Intelligence, Surveillance, and Reconnaissance
JD	Julian Day
JFCC Space	Joint Functional Component Command for Space
JHU	Johns Hopkins University
JPL	Jet Propulsion Laboratory
JPO	Joint Program Office
JSpOC	Joint Space Operations Center
LEO	Low Earth Orbit
LLA	Latitude, Longitude, and Altitude
MCS	Master Control Station
MJD	Modified Julian Day
NASA	National Aeronautic and Space Administration
NMEA	National Marine Electronics Association
NORAD	North American Aerospace Defense Command
NRL	Naval Research Laboratory
OD	Orbit Determination
ODE	Ordinary Differential Equations
P	Precise
PACS	Payload Alert Communications System
POD	Precise Orbit Determination
PPS	Precise Positioning Service
PRN	Pseudo-Random Noise
RAAN	Right Ascension of the Ascending Node
RF	Radiofrequency
RMS	Root Mean Square
RSO	Resident Space Object
SA	Selective Availability
SATCAT	Satellite Catalog
SATCOM	Satellite Communication
SBC	Single Board Computer
SBSS	Space Based Surveillance System
SERB	Space Experiments Review Board
SGP4	Simplified General Perturbations Number 4

SI	International System
SOS	Space Object Self-Tracker
SP	Special Perturbations
SPS	Standard Positioning Service
SSA	Space Situational Awareness
SSN	Space Surveillance Network
SST	Satellite-to-satellite tracking
STK	Systems Toolkit
STP	Space Test Program
STP-SIV	Space Test Program Standard Interface Vehicle
SVD	Singular Value Decomposition
SWAP	Size, Weight, and Power
TE	Temps des Ephemerides
TIMED	Thermosphere, Ionosphere, Mesopsphere Energetics and Dynamics
TLE	Two Line Element Set
TOA	Time of Arrival
TOPEX	Topography Experiment
U.S.	United States
UMT	User Motion
USAF	United States Air Force
USSC	United States Strategic Command
UT	Universal Time
UTC	Coordinated Universal Time

Bibliography

1. C. M. A. Baird, "Maintaining Space Situational Awareness and Taking it to the Next Level," *Air & Space Power Journal*, vol. September-, pp. 50–72, 2013.

2. B. Weeden, "Going Blind: Why America is on the Verge of Losing its Situational Awareness in Space and What can be Done About it," Secure World Foundation, Tech. Rep.

3. Union of Concerned Scientists, "UCS Satellite Database." [Online]. Available: http://www.ucsusa.org/nuclear{_}weapons{_}and{_}global{_}security/solutions/spaceweapons/ucs-satellite-database.html

4. M. Garcia, "Space Debris and Human Spacecraft." [Online]. Available: http://www.nasa.gov/mission{_}pages/station/news/orbital{_}debris.html

5. D. G. H. McCall and J. H. Darrah, "Space Situational Awareness: Difficult, Expensive - and Necessary," *Air & Space Power Journal*, no. Senior Leadership Perspective, pp. 6–16.

6. Vandenberg Air Force Base, "Joint Functional Component Command for Space Fact Sheet." [Online]. Available: http://www.vandenberg.af.mil/library/factsheets/factsheet.asp?id=12579

7. W. E. Wiesel, *Modern Orbit Determination*. Beavercreek, OH: Aphelion Press, 2010.

8. ——, *Modern Astrodynamics*. Beavercreek, OH: Aphelion Press, 2010.

9. M. M. Morton and T. Roberts, "Joint Space Operations Center (JSpOC) Mission System (JMS)," Situational Awareness and C2 Division, Directorate of Requirements, Headquarters Air Force Space Command, Tech. Rep., 2011.

10. T. B. Company, Ball Aerospace and Technologies Corporation, and U. Space and Missiles Systems Center, "Space Based Space Surveillance: Revolutionizing Space Awareness," 2010.

11. CSRA, "Space Object Self-Tracker Experiment ConOps."

12. D. N. Jenson, "Space Object Self-Tracker Experiment Design and Analysis," Ph.D. dissertation, Air Force Institute of Technology, Wright-Patterson AFB, OH, 2015.

13. M. A. Schaffer, "Space Object Self-Tracker Experiments," Ph.D. dissertation, Air Force Institute of Technology, Wright-Patterson AFB, OH, 2014.

14. L. B. Bastow, "Modeling the Impact of the Payload Alert Communications System (PACS) on the Accuracy of Conjunction Analysis," Ph.D. dissertation, Air Force Institute of Technology, Wright-Patterson AFB, OH, 2013.

15. D. E. Swenson, "Space Object Self-Tracker Poster," Wright-Patterson AFB, OH.

16. T. Smith, "NASA Green Propellant Infusion Mission Demonstration Project," NASA Marshall Space Flight Center.

17. C. McLean and B. Marotta, "GPPS Concept of Operations."

18. B. Porter, "CDRL 027, GPIM TO SOS PL INTERFACE CONTROL DOCUMENT," Ball Aerospace and Technologies Corporation, Boulder, CO, Tech. Rep.

19. D. E. Swenson, "Space Object Self-Tracker (SOS) Pre-Ship Review," Wright-Patterson AFB, OH.

20. NASA Orbital Debri Program Office, "Orbit Debris Graphics." [Online]. Available: http://orbitaldebris.jsc.nasa.gov/photogallery/beehives.html{\#}leo

21. M. Gruss, "Space Fence Shutdown Expected To Weaken Orbit Surveillance Network." [Online]. Available: http://spacenews.com/36720space-fence-shutdown-expected-to-weaken-orbit-surveillance-network/

22. Los Angeles Air Force Base, "Global Positioning Systems Directorate." [Online]. Available: http://www.losangeles.af.mil/library/factsheets/factsheet.asp?id=5311

23. Official United States Air Force Website, "Global Positioning System." [Online]. Available: http://www.af.mil/AboutUs/FactSheets/Display/tabid/224/Article/104610/global-positioning-system.aspx

24. National Coordination Office for Space-Based Position Navigation and Timing, "Space Segment." [Online]. Available: http://www.gps.gov/systems/gps/space/

25. R. W. Sturdevant, "NAVSTAR, The Global Positioning System: A Sampling of Its Military, Civil, and Commercial Impact," in *Societal Impact of Spaceflight*. Washington, DC: NASA History Divisiom, Office of External Relations, 2007, pp. 331–351.

26. E. D. Kaplan and C. J. Hegarty, *Understanding GPS: Principles and Applications, Second Edition*. Norwood, MA: Artech House, Inc., 2006.

27. 50th Space Wing Public Affairs, "50 SW completes GPS constellation expansion." [Online]. Available: http://www.schriever.af.mil/news/story{_}print.asp?id=123260251

28. J. Raquet, "Class Notes, "Navigation Using the GPS"," Wright-Patterson AFB, OH, 2015.

29. National Coordination Office for Space-Based Position Navigation and Timing, "Control Segment." [Online]. Available: http://www.gps.gov/systems/gps/control/

30. M. Garcia-Fernandez and O. Montenbruck, "Low Earth Orbit Satellite Navigation Errors and Vertical Total Electron Content in Single-frequncy GPS Tracking," *Radio Science*, vol. 41, no. 5, pp. 1–7, 2006.

31. P. Schwintzer, Z. Kang, C. Reigber, and S. Y. Zhu, "GPS Satellite-to-Satellite Tracking for TOPEX/Poseidon Precise Orbit Determination and Gravity Field Model Improvement," *Journal of Geodynamics*, vol. 20, no. 2, pp. 155–166, 1995.

32. F. H. Bauer, K. Hartman, and E. G. Lighsey, "Spaceborne GPS Current Status and Future Visions," in *AIAA Defense and Civil Programs Conference and Exhibit*, Huntsville, AL.

33. J. Kim and B. D. Tapley, "Error Analysis of a LowLow Satellite-to-Satellite Tracking Mission," *Journal of Guidance, Control, and Dynamics*, vol. 25, no. 6, pp. 1100–1106.

34. R. Simmons, "Class Notes, "Introductory Spaceflight Dynamics"," Wright-Patterson AFB, OH, 2014.

35. H. W. Sorenson, "Least-squares estimation from Gauss to Kalman," *IEEE Spectrum*, pp. 63–68.

36. F. R. Hoots and R. L. Roehrich, "Spacetrack Report NO. 3: Models for Propagation of NORAD Element Sets," Defense Documentation Center, Alexandria, VA, Tech. Rep.

37. Air Force Space Command, "AFSPC AStrodynamic Standard Software." [Online]. Available: http://www.afspc.af.mil/shared/media/document/AFD-130513-064.pdf

38. D. A. Vallado and P. Crawford, "SGP4 Orbit Determination," in *AIAA/AAS Astrodynamics Specialist Conference*, Honolulu, HI, 2008.

39. S. Lee, B. E. Schutz, and P. A. M. Abusali, "Hybrid Precise Orbit Determination Strategy by Global Positioning System Tracking," *Journal of Spacecraft and Rockets*, vol. 41, no. 6, pp. 997–1009, 2004.

40. J. Peláez, J. M. Hedo, and P. R. de Andrés, "A special perturbation method in orbital dynamics," *Celestial Mechanics and Dynamical Astronomy*, vol. 97, no. 2, pp. 131–150.

41. D. D. McCarthy, "Evolution of Timescales from Astronomy to Physical Metrology," Metrologia 48, US Naval Observatory, Tech. Rep.

42. R. A. Nelson, D. D. McCarthy, S. Malys, J. Levine, B. Guinot, H. F. Fliegel, R. L. Beard, and T. R. Bartholomew, "The leap second: its history and possible future," *Metrologia*, vol. 38, no. 6, pp. 509–529, 2001.

43. The Nautical Almanac Offices of the United Kingdom and the United States of America, "Systems of Time Measurement," in *Explanatory Supplement to the Astronautical Ephemeris and the American Ephemeris and Nautical Almanac*. London, England: Her Majesty's Stationery Office, 1961, pp. 66–95.

44. Time and Date, "What's a Leap Second." [Online]. Available: http://www.timeanddate.com/time/leapseconds.html

45. G. M. R. Winkler, "Modified Julian Day." [Online]. Available: http://tycho.usno.navy.mil/mjd.html

46. Department of Oceanography: Naval Postgraduate School, "Time Systems and Dates - GPS Time," 2000. [Online]. Available: http://www.oc.nps.edu/oc2902w/gps/timsys.html

47. Naval Meteorology and Oceanography Command, "GPS Week Number Rollover." [Online]. Available: http://www.usno.navy.mil/USNO/time/gps/gps-week-number-rollover

48. United States Coast Guard Navigation Center, "NAVSTAR GPS User Equipment Introduction," Alexandria, VA, Tech. Rep.

49. Naval Meteorology and Oceanography Command, "GPS Timing Data and Information." [Online]. Available: http://www.usno.navy.mil/USNO/time/gps/gps-timing-data-and-information

50. J. R. Claybrook, "Feasibility Analysis on the Utilization of the Iridium Satellite Communications Network for Resident Space Objects in Low Earth Orbit," Ph.D. dissertation, Air Force Institute of Technology, Wright-Patterson AFB, OH, 2013.

51. R. H. Newman, "Analysis and Validation of CubeSat-Class Solar Array and Battery Module," Ph.D. dissertation, Air Force Institute of Technology, Wright-Patterson AFB, OH, 2013.

52. D. A. Perry, "Space Object Self-Tracker Hardware Analysis and Environmental Testing," Ph.D. dissertation, Air Force Institute of Technology, Wright-Patterson AFB, OH, 2014.

53. J. R. Vetter, "Fifty Years of Orbit Determination: Development of Modern Astrodynamics Methods," *Johns Hopkinds APL Technical Digest*, vol. 27, no. 3, pp. 239–252, 2007.

54. N. J. P. Laboratory, "GIPSY-OASIS." [Online]. Available: https://gipsy-oasis.jpl.nasa.gov/

55. K. Kaniuth and C. Volksen, "Comparison of the BERNESE and GIPSY / OASIS II Software Systems Using EUREF Data," pp. 314–319.

56. A. P. M. Chiaradia, H. K. Kuga, and A. F. B. d. A. Prado, "Onboard and Real-Time Artificial Satellite Orbit Determination Using GPS," *Mathematical Problems in Engineering*, vol. 2013.

57. T. V. Helleputte and P. Visser, "GPS based orbit determination using accelerometer data," *Aerospace Science and Technology*, vol. 12, pp. 478–484, 2008.

58. NASA Goddard Space Flight Center, "GPS-Enhanced Onboard Navigation System (GEONS)," 2006. [Online]. Available: itpo.gsfc.nasa.gov/downloads/featured.../gsc{_}14687{_}1{_}geons.pdf

59. D. Y. Kusnierkiewicz, "An Overview of the TIMED Spacecraft," *Johns Hopkinds APL Technical Digest*, vol. 24, no. 2, pp. 150–155, 2003.

60. The Johns Hopkins University Applied Physics Laboratory, "Thermosphere, Ionosphere, Mesosphere Energetics and Dynamics," 2001.

61. NovAtel Inc., "OEM6 Family Firmware Reference Manual," Tech. Rep.

62. Analytical Graphics Inc., "STK 10 Help: Two-Body, J2 Perturbation & J4 Perturbation Propagators." [Online]. Available: http://www.agi.com/resources/help/online/stk/10.1/index.html?page=source/stk/vehSat{_}orbitProp{_}2bodyJ2J4.htm

63. J. J. Sellers, "Earth's Oblateness - J2." [Online]. Available: http://www.agi.com/resources/educational-alliance-program/astro-primer/primer91.htm

64. Analytical Graphics Inc., "STK 10 Help: High-Precision Orbit Propagator (HPOP)." [Online]. Available: http://www.agi.com/resources/help/online/stk/10.1/index.html?page=source{\%}2Fstk{\%}2FvehSat{_}orbitProp{_}2bodyJ2J4.htm

65. K. Burnett, "Precessing positions from B1950 to J2000." [Online]. Available: http://www.stargazing.net/kepler/b1950.html

66. "Latitude." [Online]. Available: https://en.wikipedia.org/wiki/Latitude

67. World Meterological Organization, "Satellite: STPSat-3," 2016. [Online]. Available: http://www.wmo-sat.info/oscar/satellites/view/541

REPORT DOCUMENTATION PAGE

Form Approved
OMB No. 0704–0188

1. REPORT DATE *(DD–MM–YYYY)*	2. REPORT TYPE	3. DATES COVERED *(From — To)*
24–03–2016	Master's Thesis	May 2015 - March 2016

4. TITLE AND SUBTITLE

Space Object Self-Tracker On-Board Orbit Determination Analysis

5a. CONTRACT NUMBER

5b. GRANT NUMBER

5c. PROGRAM ELEMENT NUMBER

6. AUTHOR(S)

Flamos, Stacie M., Civilian, USAF

5d. PROJECT NUMBER

5e. TASK NUMBER

5f. WORK UNIT NUMBER

7. PERFORMING ORGANIZATION NAME(S) AND ADDRESS(ES)

Air Force Institute of Technology
Graduate School of Engineering and Management (AFIT/EN)
2950 Hobson Way
WPAFB OH 45433-7765

8. PERFORMING ORGANIZATION REPORT NUMBER

AFIT-ENY-MS-16-M-209

9. SPONSORING / MONITORING AGENCY NAME(S) AND ADDRESS(ES)

Attn: Dr. Gregory Spanjers (ST), Chief Scientist
Space Vehicle Directorate, Air Force Research Laboratory
3350 Aberdeen Avenue SE
Albuquerque, NM 87117-5776
gregory.spanjers@us.af.mil

10. SPONSOR/MONITOR'S ACRONYM(S)

AFRL/RV

11. SPONSOR/MONITOR'S REPORT NUMBER(S)

12. DISTRIBUTION / AVAILABILITY STATEMENT

Distribution Statement A. APPROVED FOR PUBLIC RELEASE; DISTRIBUTION UNLIMITED

13. SUPPLEMENTARY NOTES

This material is declared work of the U.S. Government and is not subject to copyright protection in the United States.

14. ABSTRACT

Due to the United States' growing dependence on space based assets and the increasing number of resident space objects (RSO), improvement of Space Situational Awareness (SSA) capabilities is more necessary than ever. As a way to aid in this need, the Air Force Institute of Technology (AFIT) is developing the Space Object Self-Tracker (SOS) as a proof-of-concept experimental satellite for RSO precision tracking and collision avoidance system in Low Earth Orbit (LEO). Specifically, SOS will use Global Positioning System (GPS) position estimates for on-board orbit determination. Currently, SOS will use the Simplified General Perturbations-4 (SGP4) algorithm as its orbit determination algorithm. This research investigates the use of a modified Special Perturbations (SP) orbit determination algorithm as an alternative means for on-board orbit determination (OD) for the SOS experiment. The research is focused on evaluating performance gains and studying the effects of using GPS navigation solutions as the input observation data on the achievable accuracy of the SP algorithm. The SP OD algorithm was evaluated in testing both simulated and real world observation data. The position estimates generated by the SP algorithm from both GPS navigation solution observations and observations delivered in the J2000 inertial frame were analyzed to determine the effects of the SP algorithm's achievable performance. The accuracy of position estimates generated from the SP algorithm were also compared to those generated by SGP4 algorithm. Analysis leads to the conclusion that the SP algorithm will be beneficial in providing more accurate position estimates for observed GPS navigation solutions. However, the SP algorithm will require improvements to the dynamics modeled in the SP algorithm by specifically including more perturbations such as those due to air drag.

15. SUBJECT TERMS

Orbit Determination, Special Perturbations, SGP4

16. SECURITY CLASSIFICATION OF:			17. LIMITATION OF ABSTRACT	18. NUMBER OF PAGES	19a. NAME OF RESPONSIBLE PERSON
a. REPORT	b. ABSTRACT	c. THIS PAGE			Dr. Eric D. Swenson, AFIT/ENY
U	U	U	U	119	19b. TELEPHONE NUMBER *(include area code)* (937)255-3636 x.7479; eric.swenson@afit.edu